Level and decay scheme studies in ^{92}Zr and ^{94}Zr via $(n, n'\gamma)$ reactions*

G. P. Glasgow,† F. D. McDaniel,‡ J. L. Weil, J. D. Brandenberger,§ and M. T. McEllistrem
Department of Physics and Astronomy, University of Kentucky, Lexington, Kentucky 40506
(Received 20 March 1978)

Measurements of $(n,n'\gamma)$ excitation functions were made for incident neutron energies from 2.2 to 3.7 MeV. For ^{92}Zr, 51 transitions from 26 levels through 3472.0 keV excitation energy were observed. The ^{94}Zr study of 20 levels through 3361.2 keV excitation energy produced 28 observed γ rays, 12 of which were previously unidentified. Angular distributions were measured at 3.2 and 3.7 MeV bombarding energies for 24 and 39 transitions respectively in ^{92}Zr and at 3.1 MeV for 18 transitions in ^{94}Zr. Two new levels were discovered in ^{92}Zr at 2903.8 and 3407.9 keV. A previously reported ambiguity involving 2^+ and 4^+ levels in ^{94}Zr has been resolved, revealing a 4^+ level at 2329.0 keV and a 2^+ level at 2365.4 keV. New levels were found in this isotope at 2507.6, 2698.0, 2825.2, and 2859.8 keV. Six unique spin or spin-parity assignments, based only on the present work, were made in ^{92}Zr(E_x in keV, J^π): 2339.0, 3; 2485.1, 5; 2742.6, 4; 2903.8, 0; 3056.5, 2; 3370.9, 1; and three in ^{94}Zr: 2365.4, 2; 2507.6, 3; 2603.7, (5). A 4^-, 5^- excited proton doublet appears to have been found in each of the isotopes at excitation energies comparable to those for the doublet in ^{90}Zr. This suggests similar proton configurations for all three isotopes. Neutron inelastic scattering cross sections are in agreement with those from experiments employing neutron detection.

[NUCLEAR REACTIONS ^{92,94}Zr$(n,n'\gamma)$, E = 2.2–3.7 MeV; measured E_γ, $\sigma(E;E_\gamma, 90°)$, $\sigma(E_\gamma,\Theta_\gamma)$. Calculated $\sigma(n')$, $\sigma(E_\gamma,\Theta_\gamma)$, with statistical model. ^{92,94}Zr deduced levels, $\sigma(n')$, δ, J, π, branching ratio. Enriched targets, Ge(Li) detectors, time-of-flight background suppression.]

I. INTRODUCTION

This paper reports the results of ^{92,94}Zr$(n,n'\gamma)$ experiments to measure the energies, excitation functions, angular distributions, and branching ratios of the deexcitation γ rays of these isotopes. The experiments consisted of γ-ray excitation function measurements on each isotope using neutrons with energies from 2.2 to 3.7 MeV and angular distribution measurements at incident neutron energies of 3.20 and 3.70 MeV for ^{92}Zr and at 3.10 MeV for ^{94}Zr. From this information the ^{92}Zr and ^{94}Zr level structures near and above 2.4 MeV have been deduced and the spins of most levels either uniquely determined or limited to a few choices. γ-ray multipole mixing ratios were also obtained for many of the γ rays. Some of the present results have already been discussed in preliminary reports.[1]

Previously the level scheme for each isotope was well established to an excitation energy of 2.3 MeV, which included only 7 levels in each one. Above that energy substantial discrepancies existed in many of the reported level energies, as well as in proposed spin and parity assignments.

Kocher and Horen's[2] compilation for ^{92}Zr includes an updated level scheme, based on their evaluation of reported studies.[3-10] The energies in keV and the spins and parities of the levels below 2.0 MeV adopted by these compilers[2] are 934.46, 2^+; 1383.0, 0^+; 1495.6, 4^+; and 1847.3, 2^+. The compilers note that above 2.4 MeV, the correspondence between the levels observed in these experiments[3-10] is not good, primarily because of imprecise energy determinations in the reaction studies. Spins have been adopted[2] for only four of the levels above 2.4 MeV, and all are tentative. Figure 1 shows the adopted levels[2] above 2.0 MeV, as well as the level scheme from a recent thermal neutron capture study,[11] reviewed by Wood[12] as work in progress, and not included in the compilation.[2] These data were not available when the present study began. For comparison, the level scheme determined from the present study is also shown.

Kocher's[13] compilation for ^{94}Zr based on reported studies[3,4,7,9,10,14-18] indicated a situation similar to that for ^{92}Zr. The energies in keV and the spins and parities of the levels of ^{94}Zr below 2 MeV adopted by Kocher[13] are 918.24, 2^+; 1299.99, 0^+; 1468.34, 4^+; and 1668.74, 2^+. Figure 2 shows the level scheme above 2.0 MeV adopted by the compiler[13] and the results of the present study. Only two spins had been assigned[4,9,13] to the several levels above 2.4-MeV excitation energy prior to the present work. Singh, Taylor, and Tiven[19] have published a more complete study of ^{94}Zr from ^{94}Y decay since Kocher's compilation appeared, and this is also shown in Fig. 2, as are the results of Tessler and Glickstein.[15]

A puzzle exists in the reported ^{94}Zr level structure near 2.4 MeV. Tessler and Glickstein[15] note that the ^{94}Zr$(n,n'\gamma)$ ^{94}Zr reaction excited a 4^+ level not observed in ^{92}Zr(t,p) ^{94}Zr and ^{96}Zr(p,t) ^{94}Zr

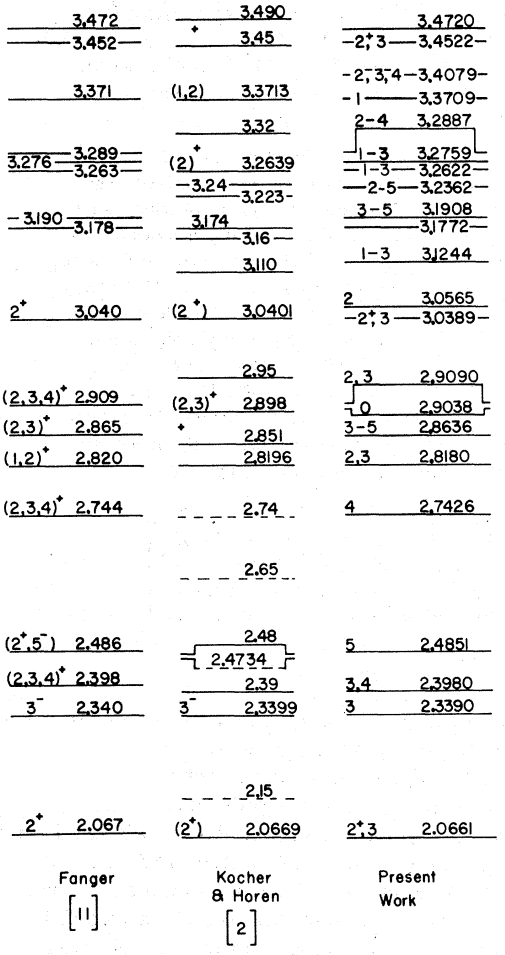

FIG. 1. A comparison of reported ^{92}Zr level schemes above 2.0 MeV. Level energies are in MeV and the J^{π} values are to the left of the levels. Author and reference number are indicated beneath each level scheme.

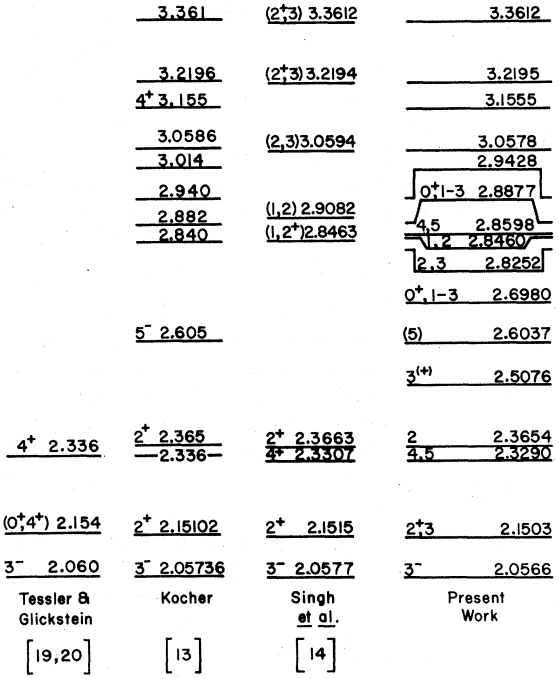

FIG. 2. A comparison of reported ^{94}Zr level schemes above 2.0 MeV. Level energies are in MeV and the J^{π} values are to the left of the levels. Author and reference number are noted beneath each level scheme.

reactions [3,4] while these latter two reactions excited a 2^+ level not observed in their $(n,n'\gamma)$ study. These results were surprising, because 2^+ levels are usually those most strongly excited in neutron inelastic scattering experiments.[20] The present study resolves these differences.

The proximity of ^{92}Zr and ^{94}Zr to neutron-shell closure at ^{90}Zr and ^{92}Mo makes them especially amenable to valence nucleon descriptions. Detailed shell model systematics of the Zr isotopes have been worked out by including proton excitations[21-23] and valence neutron excitations in the $(2d_{5/2}, 3s_{1/2})$ subshells.[24,25] The level and decay information found in this experiment can be compared directly to results of the shell model calculations.[25]

In addition to the information to be obtained about the levels of these nuclei from studying their γ-ray decays, there is considerable interest in the neutron inelastic scattering cross sections. This experiment, in fact, is one of a series[26-29] of nuclear structure and neutron scattering studies concentrated on even-A nuclei near $A = 90$. The first of the structure[26] and scattering[27] studies have been published.

There is special interest in neutron scattering cross sections in Zr because of the extensive use of this metal in reactor environments. This interest stimulated the recent $(n,n'\gamma)$ measurements on ^{90}Zr, ^{91}Zr, ^{92}Zr, and ^{94}Zr by Tessler *et al.*[14] and Glickstein *et al.*,[30] who measured excitation functions for γ rays from levels below 3-MeV excitation energy, as well as recent Argonne National Laboratory (ANL) measurements.[31] Prior to this there had been some excitation function data from earlier experiments,[16] but no data for levels above 3 MeV. No angular distributions had been measured for any of the deexcitation γ rays. Scattering cross sections inferred from the currently measured γ-ray production cross sections supplement the results obtained from neutron detection experiments completed in this laboratory[27,28] and at ANL.[31]

Neutron time-of-flight studies on separated Zr and Mo isotopes have been completed at Kentucky[26-29] for incident energies of 1.5, 2.75, 3.5, 6, and 8.6 MeV, and at ANL[31] for 13 neutron energies between 1.8 and 4.0 MeV on separated Zr isotopes. These

provide the most directly measured cross sections, but are limited in energy resolution; closely spaced levels can be resolved in the $(n,n'\gamma)$ measurements. In the present work, the inferred cross sections from γ-ray detection for well separated levels are shown to be in good agreement with those measured by direct neutron detection. (See Ref. 32 for similar comparisons.) The agreement reinforces the confidence with which the results of both detection methods are viewed.

II. EXPERIMENTAL PROCEDURES

The physical equipment and electronics used in these experiments were similar to those previously used in $(n,n'\gamma)$ studies in this laboratory.[25,26,33] Protons were accelerated by a 6.0-MeV Van de Graaff accelerator and terminal pulsed at 2 MHz with a beam pulse width of about 10 ns. The beam pulses were bunched to a 1 ns pulse width by a Mobley pulse compression system. The protons passed through a 3.61 μm molybdenum foil into 1.0 atm of tritium contained in a tantalum lined gas cell 32 mm in length and 10 mm in diameter to produce neutrons by the $T(p,n)^3$He reaction. The beam current varied from 1.0 to 2.5 μA, and the neutron energy spread was about 60 keV. The cylindrical samples were suspended in the neutron flux 50 mm from the end of the gas cell. These samples, enriched to more than 95% in a single isotope, are described in detail in Table I of Ref. 27. The ^{92}Zr sample contained 0.45 moles and the ^{94}Zr sample was 0.11 moles.

A 35 cm^3 Ge(Li) detector was 65 cm from the sample and was collimated and shielded by a cylindrical lead shell surrounded by a mixture of Li_2CO_3 and paraffin and was additionally shielded from the direct neutron flux by a 50 cm long tungsten shadow bar. The detector, collimating shield, and shadow bar were mounted on a carriage which pivoted about the scatterer. The detector energy resolution was 2.5-keV full width at half maximum (FWHM) at 1332 keV. A Hansen-McKibben long counter was located approximately 3 m from the neutron source at 90° with respect to the incident beam to monitor the neutron flux incident upon the Zr samples.

Time-of-flight techniques were used to discriminate between the prompt γ rays from neutron inelastic scattering in the samples and background γ rays. Timing methods pioneered by Gorni[34] and subsequently developed by Fouan and Passerieux[34] and by Brandenberger[33] were used to improve system resolution for wide dynamic range γ-ray detection. This dynamic range allowed γ rays from 0.1 to 3.5 MeV to be included in this experiment.

III. DATA REDUCTION

The yields of the photopeaks in 166 spectra of 4096 channels were extracted using the automatic peak fitting code SAMPO.[35] SAMPO approximates the uncertainites in the peak yields in a manner that underestimates the yield uncertainties of weak peaks.[36] Since many low yield peaks were present in these spectra, all yield uncertainties were recalculated as the rms of the foreground and background statistical uncertainties. Neutron inelastic scattering from samples of ^{19}F, ^{51}V, ^{206}Pb, and natural Fe was used to obtain the sample spectra for transitions of known energies required by SAMPO. The gain of the electronics was periodically checked using the accurately known γ rays[37] from the radioactive sources ^{152,154}Eu, ^{137}Cs, ^{60}Co, and ^{56}Co.

The yields were corrected for deadtime in the electronic counting system, attenuation, and multiple scattering of the incident neutron beam in the sample, absorption by the sample of the emitted radiation, and yield enhancement due to secondary neutron inelastic scattering. Simple analytic expressions developed for cylindrical samples by Engelbrecht[38] were used to correct for incoming neutron attenuation and multiple scattering. The product of these latter two corrections was, to within 5%, a constant for each sample for incident neutrons with energies from 2.2 to 3.7 MeV, since these are partially compensating corrections. A code previously developed in this laboratory[39] was used to correct for the absorption by the sample of the emitted γ radiation using recently measured values of the γ-ray absorption coefficients for natural zirconium and iron.[40] In this experiment the Zr yields were normalized by comparing them to those of the 847-keV transition in ^{56}Fe. In the Fe normalization measurements, neutrons with enough energy after inelastic scattering from the 847-keV ^{56}Fe level can inelastically scatter again before escaping from the sample. Each such secondary inelastic event produces a secondary 847-keV γ ray. The Engelbrecht expression[38] for neutron attenuation in the sample has been used to correct the 847-keV γ-ray yields for these contributions. Similar corrections were made to the affected γ-ray yields in the ^{92}Zr and ^{94}Zr angular distribution data.

The relative efficiency of the 35 cm^3 Ge(Li) detector was measured by the technique[41] of using radioactive sources ^{60}Co, ^{88}Y, ^{180}Ta, ^{152,154}Eu, ^{133}Ba, and ^{56}Co, which collectively emit γ rays with known energies from 300 to 2600 keV and with accurately known relative intensities.[37,42] The relative efficiency ϵ is expressed as

$$\ln(\epsilon) = 1.122 \ln(1/E_\gamma) + 0.122 [\ln(1/E_\gamma)]^2 ,$$

with E_γ in MeV. The relative efficiency uncertainties were 2% for $500 \leq E_\gamma \leq 1500$ keV, 3% for $400 \leq E_\gamma \leq 500$ keV, and $1500 \leq E_\gamma < 2500$ keV, and 4% for those from $300 \leq E_\gamma \leq 400$ keV and $2500 \leq E_\gamma$

$\leq$ 3500 keV. The ^{56}Co spectra also gave the energy dependence of R'', the yield ratio of a double escape peak to that of the full energy peak,[43] which was used to help identify double escape peaks in the ^{92}Zr and ^{94}Zr spectra.

Excitation functions at 90° of the absolute differential cross sections of the Zr γ rays were calculated by normalization to the known production cross sections of the 847-keV γ from ^{56}Fe$(n,n'\gamma)$ ^{56}Fe using the formula

$$\sigma_\gamma(E,90°)=\frac{Y_\gamma}{Y_{847}}\frac{N_{847}}{N_\gamma}\frac{\epsilon_{847}}{\epsilon_\gamma}\times\frac{M_{847}}{M_\gamma}\frac{A_{847}}{A_\gamma}\sigma_{847}(E,90°),$$

where for the Zr measurements

Y_γ = γ-ray yield corrected for deadtime,
N_γ = nuclei/cm^2 of isotope being excited,
ϵ_γ = detector relative efficiency,
M_γ = monitor counts,
A_γ = correction for neutron flux attenuation and multiple scattering and for γ-ray self-absorption,
E = incident neutron energy.

The ^{56}Fe production cross sections $\sigma_{847}(E,90°)$ were taken from an updated compilation,[44] an earlier version of which has been published.[45] The uncertainties in the Zr absolute γ-ray production cross sections were obtained by combining both the Zr photopeak yield and 847-keV photopeak yield uncertainties with the following uncertainties: detector relative efficiency, 2–4%; monitor and electronic stability, 2%; sample γ-ray self-absorption, 1%; and multiple scattering and attenuation of the incoming beam, 3–4%. The resulting uncertainties were then combined rms with the estimated 8% uncertainty in the 847-keV production cross section (see Appendix A) to give the absolute uncertainty in $\sigma_\gamma(90°)$.

Uncertainties shown in the γ-ray angular distributions include only those contributions which are angle dependent. These include statistical, deadtime, and γ-ray self-absorption correction uncertainties, and the monitor and electronic instability uncertainty. The corrected yields with their uncertainties were fitted with even-order Legendre polynomial expansions, and the resulting $4\pi A_0$ values were multiplied by the angle-independent factors and yield corrections to give the final values of σ_γ. The uncertainties in the $4\pi A_0$ values were combined rms with the angle-independent factor uncertainties to give the uncertainties in the integrated cross sections.

The neutron inelastic scattering cross section $\sigma_{n'}$ for a level was inferred by subtracting the angle-integrated production cross sections σ_γ of the γ rays feeding the level from the sum of the cross sections of γ rays depopulating the level. The uncertainties in these neutron cross sections are the rms of the production cross section uncertainties, excluding the normalization uncertainties common to all. Resulting uncertainties were then combined rms with the normalization uncertainties to give the estimated total uncertainties in $\sigma_{n'}$, the inferred neutron cross sections.

IV. RESULTS

^{92}Zr and ^{94}Zr γ-ray excitation functions

The techniques in use at Kentucky for excitation function measurements have been described.[25,45] γ-ray yields measured in 50-keV steps as a function of incident energy are extrapolated back to threshold to identify the decaying level. The thresholds plus accurately measured transition energies fix the level energy unambiguously. The advantages of the method are the lack of dependence of the detection efficiency upon neutron energy, and the fact that one can work very close to threshold, since neutrons easily enter and leave the nucleus. Accurately measured ground-state transition energies and sums of the cascade γ-ray energies usually determine the level energies to less than 1 keV.

Figures 3 and 4 display $(n,n'\gamma)$ spectra at 3.70 MeV for each isotope. Unmarked γ-ray peaks correspond to known background photopeaks. Spectra obtained in this study were characterized by good energy resolution and most peaks were well resolved from neighboring peaks and background lines. Many of the weaker peaks were more clearly visible at lower bombarding energies and many would be more visible on expanded scales. One notes the characteristic dominance of transitions from spin 2 levels, such as the 560.7- and 1132.0-keV lines in ^{92}Zr and the 1671.8-keV line in ^{94}Zr. The strongest line in ^{94}Zr at 918.3 keV has been omitted from the figure to permit a more expanded plotting scale. It seems clear also that the ^{94}Zr spectrum is substantially less complex than that of ^{92}Zr.

Figures 5, 6, and 7 display the ^{92}Zr 90° γ-ray excitation functions for the lines decaying from levels through 3472.0 keV. Figures 8, 9, and 10 display similar data measured for the γ rays decaying from the levels of ^{94}Zr through 3361.2 keV. The uncertainties shown on a particular excitation function are typical of those at most points well above the threshold of that excitation function. The γ-ray energies shown near the data are in keV and are those measured in this study. Dashed curves are guides, not fits, to the data. The excitation functions of the intense γ rays from the levels of ^{92}Zr and ^{94}Zr below 2.4 MeV, in Figs. 5 and 8, have previously been measured and measurements

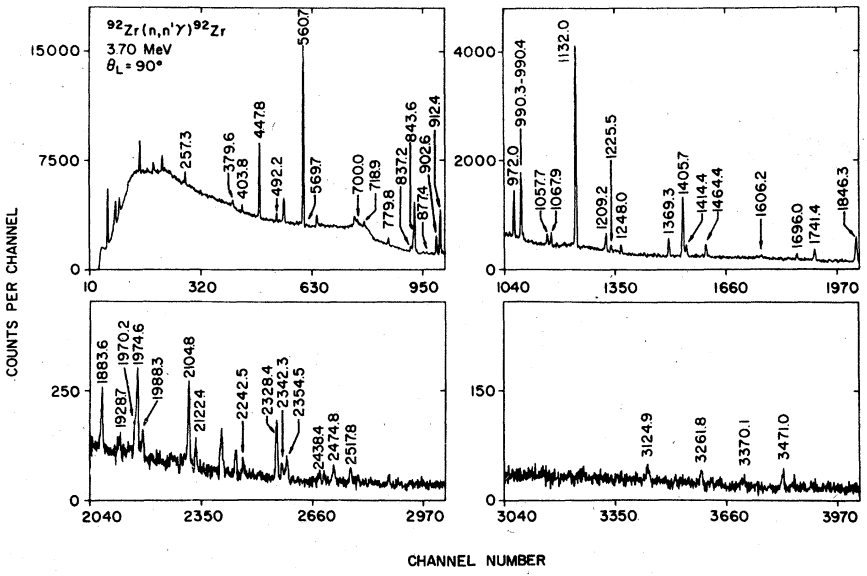

FIG. 3. A ^{92}Zr $(n,n'\gamma)$ ^{92}Zr spectrum at E_n = 3.70 MeV and θ = 90°. ^{92}Zr γ-ray energies are in keV and unlabeled peaks represent background or unidentified peaks. The dominant peak, 934.1 keV, in channel 1020, has been suppressed to emphasize the other peaks in the spectrum.

of their thresholds were not made in this study.

The ^{92}Zr γ-ray energies, level energies, and uncertainties determined from this study are compared in Table I to those reported from the β-decay studies included in Ref. 2 and from a recently reported neutron capture study.[11] The six γ rays, as identified in previous $(n,n'\gamma)$ studies,[14,16] are all from the well-known lower energy levels of ^{92}Zr and are not included in Table I. Table II compares similar data for ^{94}Zr to that adopted by Kocher[13] from the results of various ^{94}Y β-decay experiments and $(n,n'\gamma)$ studies.[14-19]

Tables I and II and the accompanying excitation functions give several new γ rays and energy levels identified in the present experiment. The ^{92}Zr results agree with those of Fanger *et al.*[11] and confirm the energies of many of the γ rays reported in that study.

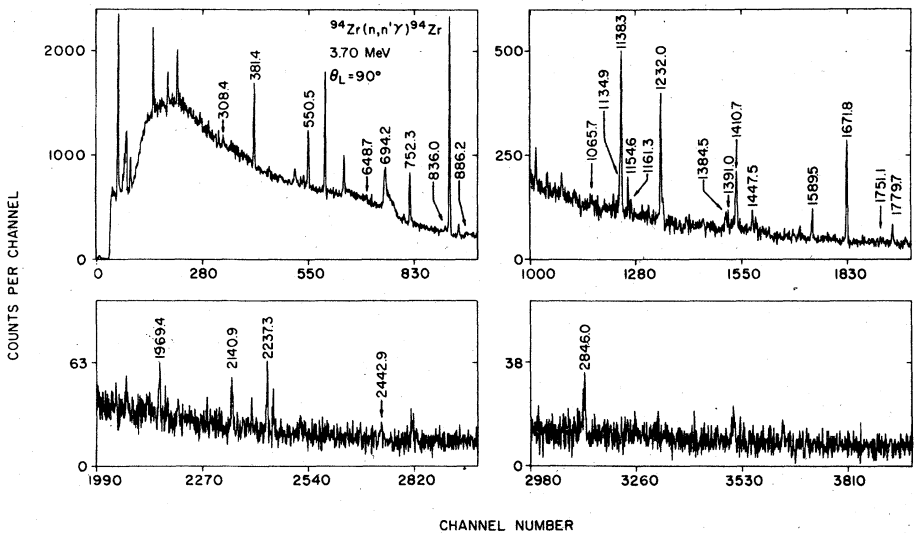

FIG. 4. A ^{94}Zr $(n,n'\gamma)$ ^{94}Zr spectrum at E_n = 3.70 MeV and θ = 90°. The dominant peak in the spectrum, 918.3 keV, in channel 1000, has been suppressed to emphasize the other peaks. Other comments in the caption of Fig. 3 also apply to this figure.

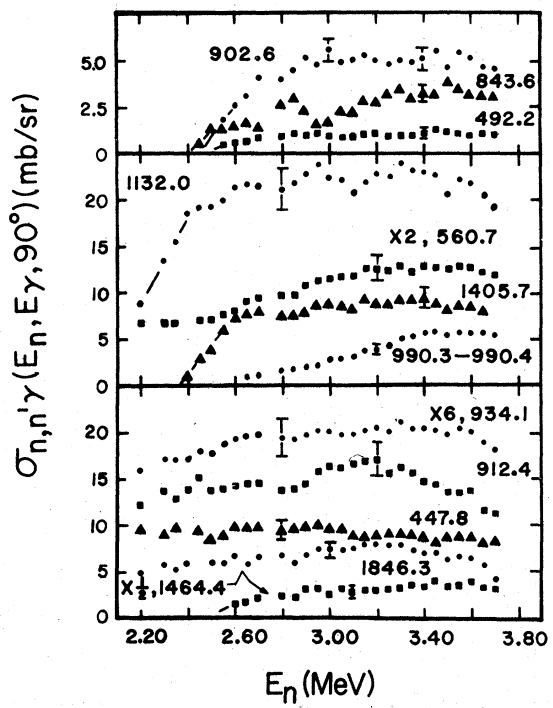

FIG. 5. Excitation functions of the deexcitation γ rays of ^{92}Zr. The uncertainties shown, typical of those at most points, include the normalization uncertainty. The γ-ray energies are in keV. The magnitudes of certain excitation function cross sections have been reduced for display and the displayed cross sections should be multiplied by the indicated scale factors. Dashed line curves are guides, not fits, to the data. The 990.3–990.4 excitation function is a composite of the excitation functions of the γ rays of these energies.

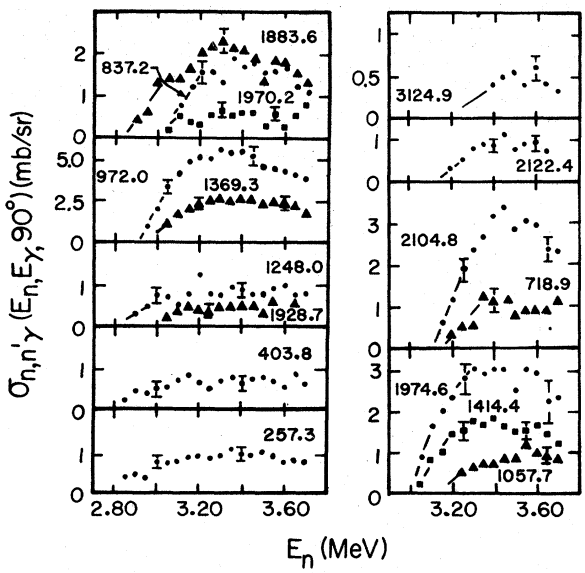

FIG. 6. Excitation functions of the deexcitation γ rays of ^{92}Zr. Comments in the caption of Fig. 5 also apply to this figure.

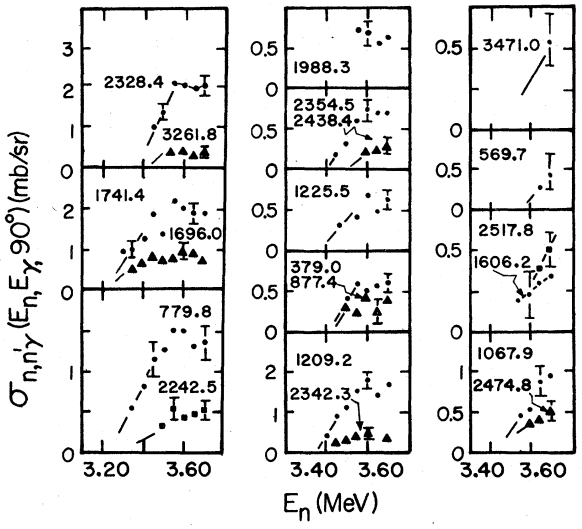

FIG. 7. Excitation functions of the deexcitation γ rays of ^{92}Zr. Comments in the caption of Fig. 5 also apply to this figure.

Analysis of the ^{92}Zr excitation functions

We have found no evidence in the present work for the proposed[2,3,5,6,8,9] levels at 2.15, 2.18, 2.474, 2.65, and 2.95 MeV. It has been suggested[2] that the tentatively proposed 2.18-MeV level was actually a ^{90}Zr contaminant line. The 2186-keV γ

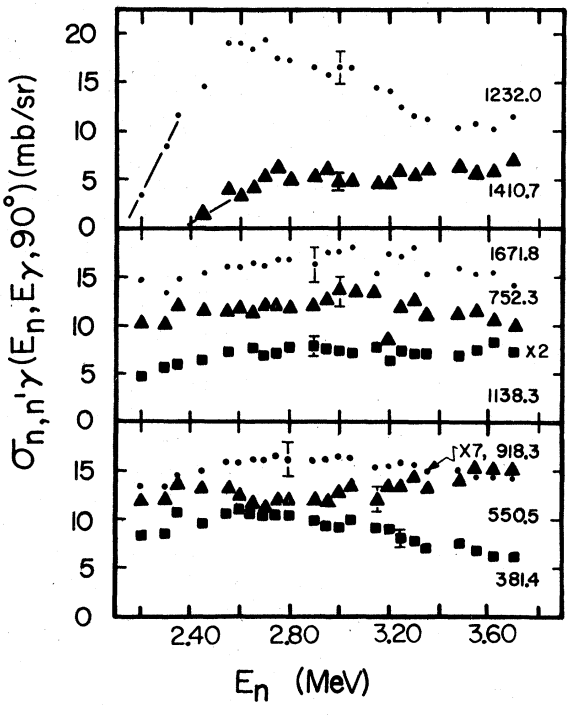

FIG. 8. Excitation functions of the deexcitation γ rays of ^{94}Zr. Comments in the caption of Fig. 5 also apply to this figure.

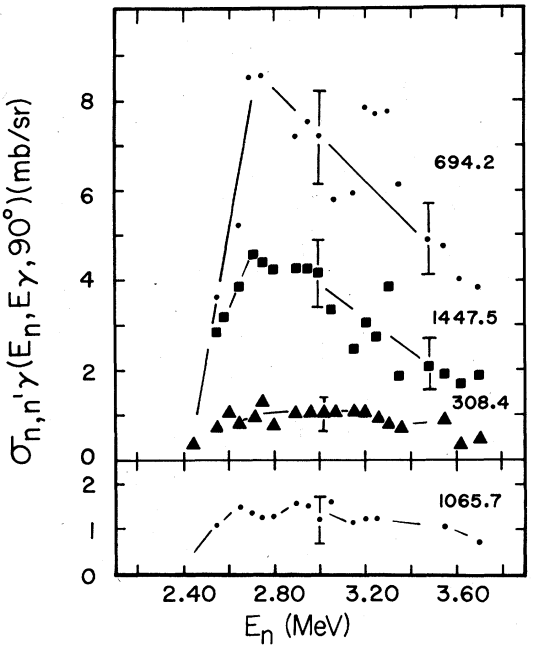

FIG. 9. Excitation functions of the deexcitation γ rays from the 2365.4-keV level of ^{94}Zr. Comments in the caption of Fig. 5 also apply to this figure.

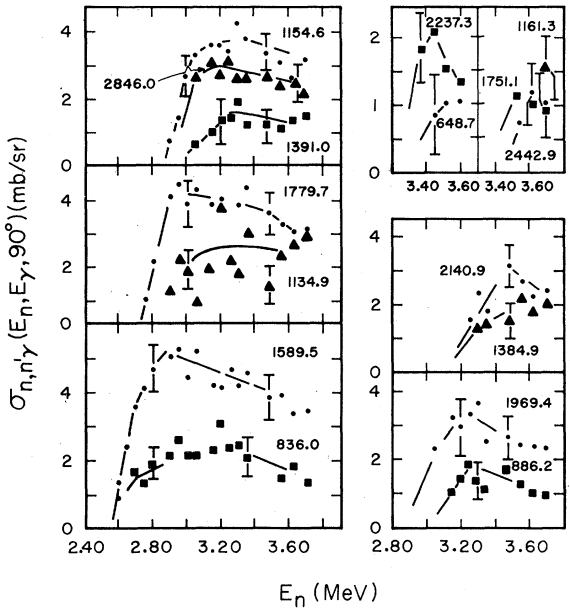

FIG. 10. Excitation functions of the deexcitation γ rays from the higher energy levels of ^{94}Zr. Comments in the caption of Fig. 5 also apply to this figure.

ray observed in both ^{92}Zr and ^{94}Zr spectra in the present work has been assigned to the 2^+ level to ground-state transition in the 2% ^{90}Zr contaminant in both samples.

Two new ^{92}Zr energy levels were found at 2903.8 and 3407.9 keV. Each level emits two γ rays to well-known low-lying levels and the good agreement of the excitation function thresholds helps establish the existence of these new levels.

The main differences between this work and that of Ref. 11, as can be seen in Table I, are that we have found more energy levels in the region up to 3.472 MeV, while for many of the levels Fanger has observed more γ rays. In particular, Fanger *et al.*[11] do not report the energy levels at 2903.8, 3056.5, 3124.4, and 3407.9 keV.

A study of the level schemes from earlier work reveals that from 2.0 to 3.3 MeV the energies assigned from the (d,p) experiment[5] are 6 to 12 keV lower than those of the present experiment and of Ref. 11, while the levels in the (t,p) studies[3] are about 6 keV high. In this energy region, the indicated adjustments in the energies reported from the (t,p) and (d,p) studies bring several level energies into agreement with these more recently measured values. These adjustments of energy scales from the transfer reaction studies are within the uncertainties assigned in those experiments, and would result in changes in several level energies in the adopted scheme of Kocher and Horen[2] as shown in Fig. 1. In particular the proposed levels at 2851, 3110, and 3223 keV would actually be the levels found here at 2863.6, 3124.4, and 3236.2 keV. The last level would correspond also to that placed at 3240 and 3247 keV in the (t,t') and (t,p) reaction studies respectively.

The only special problem with the excitation functions in ^{92}Zr worthy of note concerns the 990.3–990.4-keV transitions shown in Fig. 5. This excitation function does not show the characteristic energy dependence of statistical model cross sections for excitation of a single level, as depicted by the 1232.0-keV transition of Fig. 8, for example. It shows instead the typical behavior of strong cascade-feeding from a higher level. In this case that is not possible since no cascade transition feeding the 2485.1-keV level of sufficient strength is observed to have a threshold near 3.05–3.10 MeV, where the yield of the 990.3–990.4-keV line shows a strong increase. There is a level excited at 3056.5 keV, however, whose 718.9- and 2122.4-keV decays are shown in Fig. 6 to have a threshold near 3.1 MeV. This level can also decay to the 2066.1-keV level with a 990.4-keV line. Thus, above 3.1-MeV incident energy the 990.3-keV line becomes a 990.3–990.4-keV composite group.

The level discovered at 3407.9 keV decays by emitting 2474.8-keV and 1067.9-keV γ rays. The 2474.8-keV γ had been suggested[6] as a ground-state transition from a level of the same energy. However, our results exclude that possibility because the threshold of the 2474.8-keV excitation

TABLE I. A comparison of the ^{92}Zr γ-ray energies and level energies determined in this study to those from ^{92}Y β decay (Ref. 6) and a recent ^{91}Zr(n,γ) study (Refs. 11 and 12).

This work		Fanger *et al.* (Ref. 11)		β decay, ^{92}Y Ref. 6	
Level (keV)	E_γ (keV)	Level (keV)	E_γ (keV)	Level (keV)	E_γ (keV)
934.1 ± 0.5	934.1 ± 0.5	934.46	934.46	934.5	934.5
1381.9 ± 0.8	447.8 ± 0.6	1382.68	448.22	1383.0	448.5
1494.8 ± 0.8	560.7 ± 0.6	1495.42	560.92	1495.6	561.1
1846.4 ± 0.4		1847.24	(352.33)	1847.3	
	912.4 ± 0.5		912.76		912.8
	1846.3 ± 0.5		1847.26		1847.3
2066.1 ± 0.7		2066.6	219.2	2066.9	
			571.4		
	1132.0 ± 0.5		1132.13		1132.4
2339.0 ± 0.6		2339.60	272.9	2339.1	
	492.2 ± 0.6		492.37		492.0
	843.6 ± 0.8		844.19		844.3
	1405.7 ± 0.7		1405.16		1405.4
			(2339.6)		2339.9
2398.0 ± 0.6	902.6 ± 0.5	2398.28	902.86		
	1464.4 ± 0.7		1463.82		
2485.1 ± 0.9	990.3 ± 0.5	2486.0	990.54		
			1103.39		
2742.6 ± 0.6	257.3 ± 0.7	2743.5	257.56		
			344.79		
	403.8 ± 0.5		403.81		
			(677.4)		
	1248.0 ± 0.6		1248.08		
2818.0 ± 0.5		2819.4	333.89	2819.6	
	972.0 ± 0.5		972.33		972.3
			1436.2		
	1883.6 ± 0.5		1885.1		1885.1
			(2819.07)		2819.6
2863.6 ± 0.6	1369.3 ± 0.6	2865			
	1928.7 ± 0.2				
2903.8 ± 0.7	837.2 ± 0.8				
	1970.2 ± 0.7				
2909.0 ± 0.5		2909.3	569.5		
			842.69		
			1061.7		
	1414.4 ± 0.7		1414.05		
	1974.6 ± 0.5		1974.90		
3038.9 ± 0.8		3039.6	295.8	3040.1	
	(700.0 ± 1.0)		700.13		
			1192.5		
	2104.8 ± 0.6		2105.13		2105.6
3056.5 ± 0.7	718.9 ± 0.6				
	990.4 ± 1.0				
	2122.4 ± 0.7				
3124.4 ± 0.8	1057.7 ± 0.5				
	3124.9 ± 1.3				
3177.2 ± 1.1	779.8 ± 0.7	3178			
	2242.5 ± 1.5				
3190.8 ± 1.0	1696.0 ± 0.5	3190			
3236.2 ± 1.0	1741.4 ± 0.6				
3262.2 ± 0.6	2328.4 ± 0.5	3262.9	2328.1	3263.9	
	3261.8 ± 1.5		3262.3		3263.9
3275.9 ± 0.5		3275.7	(366.6)		
	877.4 ± 0.5		877.51		
	1209.2 ± 0.6		1209.19		
	2342.3 ± 0.7		2340.9		

TABLE I. *(Continued)*.

This work		Fanger *et al.* (Ref. 11)		β decay, ^{92}Y Ref. 6	
Level (keV)	E_γ (keV)	Level (keV)	E_γ (keV)	Level (keV)	E_γ (keV)
3288.7 ± 0.6	379.6 ± 0.5	3289.2	379.64		
			891.0		
	1225.5 ± 0.6		1222.43		
			1793.9		
	2354.5 ± 0.5		2354.8		
3370.9 ± 0.7		3371.0	1032.0	3371.3	
	1988.3 ± 0.6		1988.75		1988.6
	2438.3 ± 0.7		2436.9		2437.0
	(3370.1 ± 1.6)		3371		3371.2
3407.9 ± 0.6	1067.9 ± 0.5				
	2474.8 ± 0.6				
3452.2 ± 0.6		3452	(632.1)		
			1112.6		
	1606.2 ± 0.8		1604.85		
			1956.6		
			2069.5		
	2517.8 ± 0.6		2517.8		
3472.0 ± 1.1	569.7 ± 0.7	3472	2537.1		
	3471.0 ± 2.0		3475.2		

function, shown in the lower right panel of Fig. 7, is well above 2.474 MeV.

The last two ^{92}Zr level energies assigned in this study, 3452.2 and 3472.0 keV, agree with the 3452-keV and 3472-keV level energies reported by Fanger *et al.*[11]

Analysis of the ^{94}Zr excitation functions

This study resolves a puzzle, mentioned in the Introduction, in the ^{94}Zr level structure near 2320–2370 keV. Day and Lind[16] reported one level at 2320 keV, based on a 1.40-MeV γ-ray decay to the first excited state. Tessler *et al.*[14] concluded that a 1.45-MeV γ ray in their spectrum and Day and Lind's 1.40-MeV γ ray were the same, but that it was decaying from a level at 2360 keV with a tentative spin of (4), reported from a (p,p') study by Dickens *et al.*[9] Tessler and Glickstein[15] later corrected their γ-ray energy to 1416 keV and fixed the level at 2336 keV. After searching unsuccessfully for a 2^+ to ground-state γ ray and other possible decays from the 2^+ level reported in this energy region in the (t,p) and the (p,t) experiments,[3,4] they concluded only a 2336-keV level existed in this region.

The results of the present experiment clearly show two levels. One, the 2329.0-keV level, emits the 1410.7-keV γ ray which is apparently the same γ ray reported by Day and Lind[21] and also by Tessler and Glickstein,[15] although not at exactly this energy. This also confirms a tentative level reported at 2320 keV in the (p,p') experiment.[9] The second energy level at 2365.4 keV emits four γ rays with energies of 308.4, 694.2, 1065.7, and 1447.5 keV. The monotonically decreasing excitation functions of these γ rays, shown in Fig. 9, imply that there are only weak or perhaps no cascades to this level. The sharp decrease in their cross sections with increasing neutron energy suggests why they would not appear in the spectrum which Tessler and Glickstein[15] obtained with 5.0-MeV neutrons. In Fig. 4, the 694.2-keV photopeak is the narrow structure present on the recoil broadened 694-keV background line prominent in all $(n,n'\gamma)$ spectra measured with Ge(Li) detectors. The location of this peak on a strong background line may also explain why it was not reported in earlier studies. The use of time of flight to separate prompt γ rays from neutrons aids in resolving such structure by drastically reducing the neutron induced background lines. In the very recent work of Singh *et al.*,[19] exactly the same level structure and γ-ray transitions were found in this region of excitation.

The panels of Fig. 10 display the excitation functions of the γ rays from the ^{94}Zr levels between 2400 and 2860 keV. A previously unreported level at 2507.6 keV emits the 1589.5- and 836.0-keV deexcitation γ rays. Several authors report the 2603.7-keV level.[3,4,7,9,10]

Its 1134.9-keV γ ray appears as a small shoulder on the strong 1138-keV peak; it was only successfully resolved from that strong peak at energies

TABLE II. A comparison of the ^{94}Zr γ-ray energies and level energies determined in this study to those reported in $(n,n'\gamma)$ and ^{94}Y β decay experiments included in Ref. 13 and reported in Ref. 19.

This work		Kocher (Ref. 13) ^{94}Y β decay		Kocher (Ref. 13) $(n,n'\gamma)$		Singh (Ref. 19) ^{94}Y β decay	
Level (keV)	E_γ (keV)	Level (keV)	E_γ (keV)	Level (keV)	E_γ (keV)	Level (keV)	E_γ (keV)
918.3±0.5	918.3±0.5	918.24	918.24	920	920	918.8	918.8
1299.7±0.7	381.4±0.5	1299.99	381.75	1300	380	1300.4	381.6
1468.8±0.7	550.5±0.5	1468.34	550.10	1421	551	1469.7	550.9
1671.2±0.9	752.3±0.8	1668.74	750.52	1675	753	1671.5	752.6
	1671.8±0.8		1668.57		1675		1671.4
			(202.0)				
2056.6±0.8	1138.3±0.6	2057.36	1139.12	2060	1140	2057.7	1138.9
			588.0				588
2150.3±0.9	1232.0±0.7	2151.02	1232.78	2154	1234	2151.5	1232.6
2329.0±0.9	1410.7±0.9			2336	1416	2330.7	1411.9
2365.4±0.6	308.4±0.8	2365.5				2366.3	308.2
	694.2±1.0						694.7
	1065.7±0.5						1066.5
	1447.5±0.8		1447.3				1447.4
2507.6±0.7	836.0±0.7						
	1589.5±0.9						
2603.7±1.1	1134.9±0.8						
2698.0±1.1	1779.7±1.0						
2825.2±1.1	1154.6±0.6						
2846.0±5.0	2846.0±5.0	2834	(2834.0)			2846.3	2846.3
							1927.5
2859.8±1.3	1391.0±1.1						
2887.7±1.8	1969.4±1.7						
						2908.2	2908.4
							1989.3
							1236.6
2942.8±1.4	886.2±1.2						
3057.8±1.4	1384.9±1.0	3058.6				3059.4	
	2140.9±2.5		2140.4				2140.6
			(694.0)				
							1001.8
3155.5±1.5	648.7±0.8						
	2237.3±2.5						
3219.5±1.5	1161.3±0.7	3219.6	1162.2			3219.4	1161.8
	1751.1±1.3						
							2300.5
							887.5
3361.2±3.4	2442.9±3.4	3361.1	2444.0			3361.2	2442.1
			1892.8				1891.6
							1303.8

more than 250 keV above threshold. The 1779.7-keV γ ray locates a new level at 2698.0 keV. From their (p,p') experiment, Dickens *et al.*[9] have tentatively reported three levels in the 2800–2940-keV region. The particle transfer and inelastic scattering [3,7,10] experiments indicate only one or two levels in this region and fail to resolve all of the levels proposed by Dickens *et al.*[9] We find a level in this region at 2825.2 keV, which emits an 1154.6-keV γ ray. A 2846-keV γ ray places a level at that energy, supporting the 2845.6-keV assignment made by Cavallini *et al.*[17] A weak 1391.0-keV γ ray locates a level at 2859.8 keV. We do not find the 2834-keV level proposed by Hontzeas and Marsden.[18]

Figure 10 also contains the excitation functions of the 1969.4- and 886.2-keV γ rays from the reported levels at 2887.7 and 2942.8 keV, respectively. It appears that Singh *et al.*[19] have mistakenly concluded that the 886-keV γ ray is a transition from the level at 3219.5 keV, since it is seen here to be excited by neutrons with $E_n \simeq 3.15$ MeV. In the energy region from 3057 to 3361 keV, four levels have been observed. No prior experiment has

concurrently excited all of them. Figure 10 displays the excitation functions of the weak γ rays from these four levels. The γ rays at 202, 588, and 1892.8 keV reported in Refs. 17 and 19 and adopted by Kocher[13] were not found in this study. Neither were the three γ rays at 1237, 1989 and 2908 keV reported in Ref. 19 seen in the present study; they may have been below our limit of sensitivity.

Angular distributions of γ rays in ^{92,94}Zr

In addition to providing γ-ray branching ratios, spins or spin restrictions and γ-ray multipole mixing ratios often can be determined or at least limited by comparing the experimental angular distributions to the distributions predicted by the Wolfenstein-Hauser-Feshbach (WHF) formalism.[46] Many prior studies have shown that the spins of the decaying levels often can be determined uniquely if the anisotropies of the γ-ray angular distributions are large.[45,47] Even if the anisotropy is not large, the spin can usually be limited to a few choices. The angular distributions provide reliable tests for spin assignments because they are essentially independent of the neutron scattering mechanism. They depend on the alignments or magnet-

TABLE III. ^{92}Zr angle-integrated γ-ray production cross sections and Legendre polynomial least-squares fitting coefficients at $E_n = 3.20$ and 3.70 MeV. $\sigma_\gamma = 4\pi A_0$ unless noted otherwise.

Level (keV)	E_γ (keV)	Integrated cross sections $\sigma_\gamma(E_\gamma)$ (mb) 3.20 MeV	3.70 MeV	Legendre polynomial coefficients 3.20 MeV a_2	3.70 MeV a_2	3.70 MeV a_4
934.1	934.1	1612 ± 154	1407 ± 152	0.13 ± 0.02	0.12 ± 0.02	
1381.9	447.8	101 ± 10	85 ± 9	0.0	0.0	
1494.8	560.7	358 ± 34	336 ± 36	0.25 ± 0.03	0.22 ± 0.03	
1846.4	912.4	216 ± 21	143 ± 15	0.10 ± 0.03	0.09 ± 0.02	
	1846.3	101 ± 10	69 ± 8	0.17 ± 0.03	0.18 ± 0.02	
2066.1	1132.0	252 ± 24	223 ± 24	−0.21 ± 0.01	−0.20 ± 0.01	
2339.0	492.2	12 ± 1	10 ± 1	−0.21 ± 0.05	0.25 ± 0.17	
	843.6	37 ± 4	35 ± 4	−0.24 ± 0.05	−0.20 ± 0.07	
	1405.7	98 ± 9	89 ± 10	−0.28 ± 0.02	−0.22 ± 0.02	0.05 ± 0.03
2398.0	902.6	73 ± 7	69 ± 7	0.31 ± 0.06	0.26 ± 0.03	
	1464.4	25 ± 3	25 ± 3	0.29 ± 0.07	0.29 ± 0.07	
2485.1	990.3	38 ± 5	37 ± 10	−0.19 ± 0.03	−0.15 ± 0.02	
2742.6	257.3	9 ± 1	7 ± 1	−0.30 ± 0.11	−0.34 ± 0.12	
	403.8	8 ± 1	6 ± 1	−0.27 ± 0.07	−0.15 ± 0.13	0.54 ± 0.19
	1248.0	14 ± 1	12 ± 1	0.31 ± 0.03	0.33 ± 0.10	
2818.0	972.0	72 ± 7	51 ± 6	0.11 ± 0.03	0.14 ± 0.04	
	1883.6	27 ± 3	18 ± 2	0.0	0.0	
2863.6	1369.3	30 ± 9	29 ± 3	0.07 ± 0.03	0.0	
	1928.7	7 ± 1	8 ± 1	0.63 ± 0.15		
2903.8	837.2	15 ± 2	16 ± 2	0.0	0.0	
	1970.2	(15 ± 2) [a]	14 ± 1		0.0	
2909.0	1414.4	19 ± 2	23 ± 3	0.27 ± 0.08	0.24 ± 0.05	
	1974.6	26 ± 3	29 ± 3	−0.10 ± 0.03	0.0	
3038.9	2104.8	12 ± 1	26 ± 3	−0.35 ± 0.08	−0.34 ± 0.05	
3056.5	718.9	(5 ± 1) [a]	12 ± 1		−0.31 ± 0.06	
	990.4	(8 ± 3) [a]	(31 ± 8) [a]			
	2122.4	5 ± 1	12 ± 1	0.26 ± 0.06	0.41 ± 0.11	
3124.4	1057.7		13 ± 1		0.0	
3177.2	779.8		23 ± 3		0.27 ± 0.08	−0.24 ± 0.12
	2242.5		7 ± 1		0.0	
3190.8	1696.0		14 ± 2		0.34 ± 0.08	
3236.2	1741.4		24 ± 3		−0.24 ± 0.02	
3262.2	2328.4		27 ± 3		0.0	
3275.9	877.4		5 ± 1		0.0	
	1209.2		22 ± 2		−0.10 ± 0.04	
3288.7	379.6		8 ± 1		0.0	
	1225.5		10 ± 1		0.41 ± 0.12	
3370.9	1988.3		11 ± 1		0.0	
3407.9	1067.9		11 ± 1		−0.50 ± 0.07	
3452.2	1606.2		6 ± 1		−0.38 ± 0.10	

[a] Cross section estimate given by $4\pi\sigma_\gamma(90°)$.

ic substate populations of the levels excited in the scattering process. At low incident neutron energies these alignments reflect primarily the high l-dependent penetrabilities for the incoming and outgoing neutrons, which in turn depend primarily on the size of the nucleus and the neutron energies. Comparisons[20] of alignments and of spin assignments and limitations obtained by these angular distribution methods with results from other types of structure studies have shown the reliability of this method.

A secondary and weaker reliance can be placed on the use of cross section comparisons[16] to limit spin choices for scattering in spherical nuclei. The cross sections calculated with the WHF statistical model are good approximations to the neutron inelastic scattering cross sections at bombarding energies $E_n \leq 4$ MeV in such nuclei. The model cannot be too precise, partly because it neglects the influence of nuclear dynamics on the cross sections. Nonetheless, such comparisons have been successfully used in this [16,30] and other mass regions. Spin choices usually can be rejected if the predicted inelastic cross sections differ by a factor or greater than 2 from those inferred from the γ-ray measurements in such spherical nuclei.

Angular distributions were measured for 24 γ rays for ^{92}Zr at a neutron bombarding energy of 3.20 MeV and for 39 γ rays at 3.70 MeV. Eighteen angular distributions were measured for ^{94}Zr at an energy of 3.10 MeV. These angular distributions consisted of γ-ray yields measured at 9 equally spaced angles from 30° to 150°. Least-squares fits to the yields and their uncertainties were made with the even-order Legendre polynomial expression:

$$Y(\theta) = A_0[1 + a_2 P_2(\cos\theta) + a_4 P_4(\cos\theta)] .$$

The numbers of coefficients included in each fit was determined using the χ^2 and F_χ test least-squares fitting criteria described by Bevington.[48]

Table III lists the coefficients of the least-squares fits to the data for the ^{92}Zr distributions at each energy, as well as the angle-integrated γ-ray production cross sections. Table IV presents the ^{94}Zr

TABLE IV. The 3.10 MeV ^{94}Zr angular distribution least-squares coefficients and γ-ray production cross sections. When they occur, a_4 coefficients are listed immediately under the second order coefficient. The γ-ray production cross sections are given by $\sigma_\gamma = 4\pi A_0$.

Level (keV)	E_γ (keV)	a_2 and a_4 coefficients	$\sigma_\gamma(E_\gamma)$ (mb)
918.3	918.3	0.15 ± 0.02	1570 ± 150
1299.7	381.4	0.0	108 ± 11
1468.8	550.5	0.25 ± 0.02	204 ± 20
		−0.09 ± 0.03	
1671.2	752.3	0.0	169 ± 16
	1671.8	0.17 ± 0.02	247 ± 24
2056.6	1138.3	−0.27 ± 0.02	180 ± 17
2150.3	1232.0	−0.30 ± 0.04	190 ± 18
		−0.13 ± 0.06	
2329.0	1410.7	0.29 ± 0.09	84 ± 9
		−0.39 ± 0.13	
2365.4	308.4	0.0	10 ± 1
	694.2	0.14 ± 0.07	98 ± 10
	1065.7	0.28 ± 0.10	18 ± 2
	1447.5	0.48 ± 0.04	63 ± 6
2507.6	836.0	−1.04 ± 0.29	14 ± 2
	1589.5	0.53 ± 0.05	98 ± 10
2698.0	1779.7	0.0	53 ± 5
2825.2	1154.6	0.28 ± 0.05	56 ± 5
2859.8	1391.0	0.32 ± 0.22	22 ± 3
2887.7	1969.4	0.0	27 ± 3

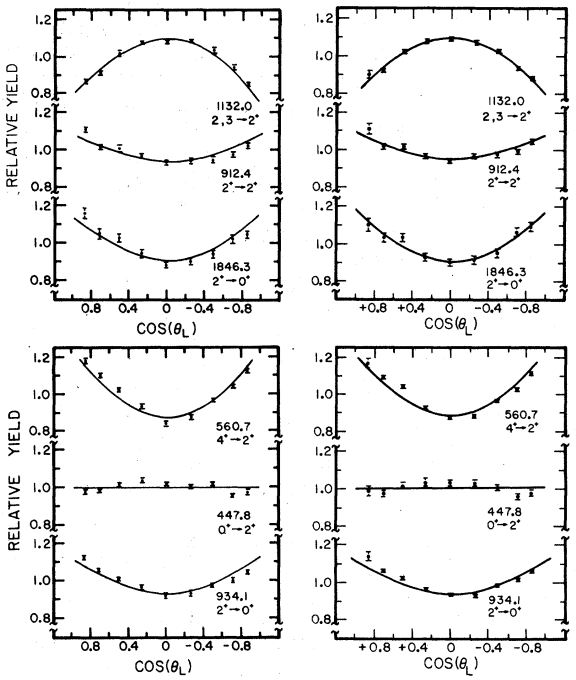

FIG. 11. The angular distributions of deexcitation γ rays of ^{92}Zr. The left panels display distributions measured at 3.20 MeV while the right panels display distributions measured at 3.70 MeV. Identifying γ-ray energies are in keV. J_f^π and J_i are noted for the two levels associated with the transition. Solid curves are least-square fits to the relative yields. Dashed curves are angular distribution shapes calculated from WHF theory for the spins indicated. When the theoretical distributions coincide with the solid curves, the dashed curves are not shown. The error bars, representing probable errors, include yield and monitor uncertainties but do not include the normalization uncertainty. Note that the scale zeros are suppressed. The initial spin possibilities, J_i given in the figure are all those which are not inconsistent with the present experimental results. Initial level parities, π_i are not given in the figures unless they have been established in earlier work because the WHF angular distributions are essentially independent of parity.

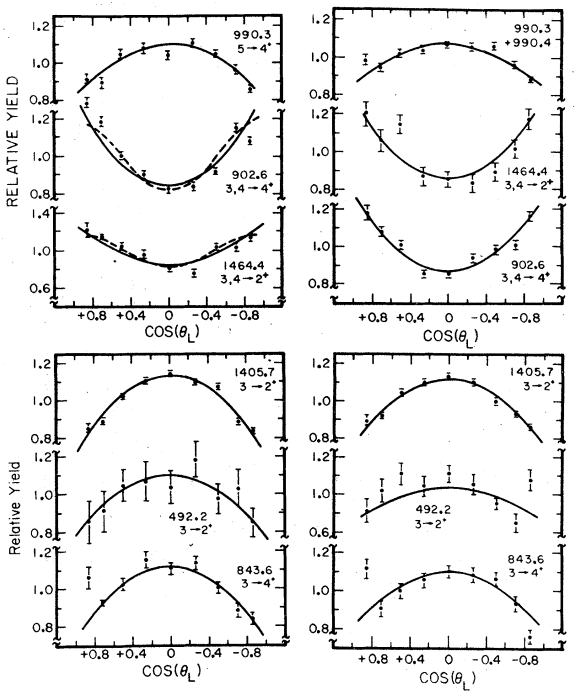

FIG. 12. The angular distributions of deexcitation γ rays of ^{92}Zr. The left panels display distributions measured at 3.20 MeV and the right panels show distributions measured at 3.70 MeV. Comments in the caption to Fig. 11 also apply to this figure.

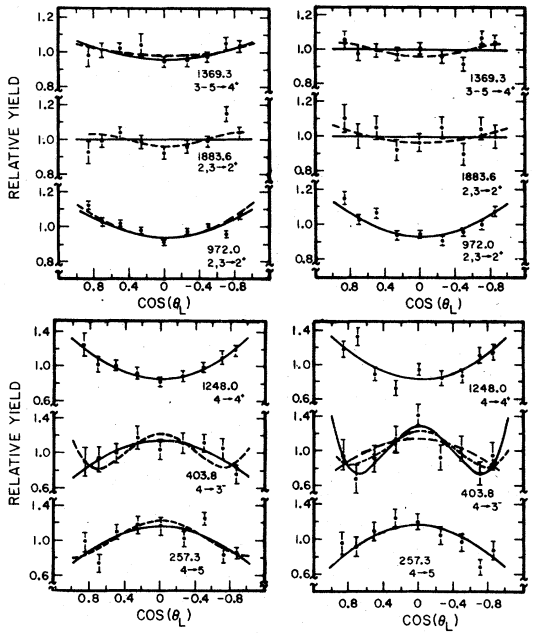

FIG. 13. The angular distributions of deexcitation γ rays of ^{92}Zr. The left panels display the distributions measured at 3.20 MeV and the right panels show distributions measured at 3.70 MeV. Comments in the caption to Fig. 11 also apply to this figure. The notation 3–5 with the 1369.3-keV angular distribution indicates that spins 3, 4, and 5 are possible spin assignments. Similar notation is used with other angular distributions in the remaining figures. Note that the relative yield scales are not all identical.

least-squares fit coefficients and γ-ray production cross sections. The statistical test information, associated with the goodness of fit tests,[48] is not presented here.

The γ-ray angular distributions for transitions in ^{92,94}Zr are shown in Figs. 11 through 19. For each distribution, both the least-squares fits (LSF) to the measurements and WHF theoretical calculations are shown. The LSF are represented as solid curves, and the WHF curves often coincide with them. When the WHF curves are different, they are shown as dashed curves. These theoretical calculations have as an adjustable parameter the mixing ratio, δ, which defines the interference between two multipole orders in the γ-ray transition. The mixing ratio was adjusted as described below to minimize the deviation of the WHF from the LSF curves. For many transitions, several spin choices for excited levels are consistent with the data of Figs. 11–19.

The WHF calculations require transmission coefficients of a complex potential appropriate to these Zr isotopes. Potentials had been determined from a first analysis of preliminary results for neutron elastic and inelastic scattering from even-A Mo isotopes,[29] and they were very similar to potentials available from Knolls Atomic Power Laboratory.[49] The ^{94}Mo and ^{96}Mo potentials[29] were used for ^{92}Zr and ^{94}Zr. They have real depths of 47.2 and 47.0 MeV, and Woods-Saxon derivative imaginary depths of 8.8 and 9.0 MeV respectively. The real and imaginary diffusenesses are 0.65 and 0.47 fm respectively, and the real and imaginary radii are $1.25A^{1/3}$ and $1.30A^{1/3}$ fm.

Using the complex potential code ABACUS-II (revised)[50] to calculate the transmission coefficients,

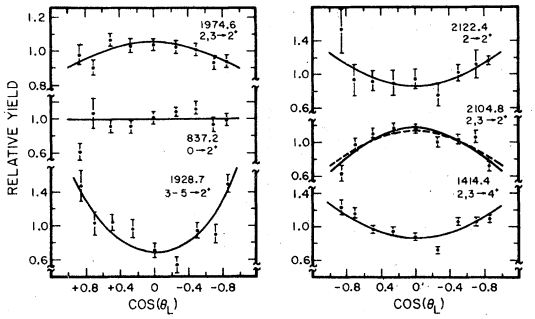

FIG. 14. Angular distributions of deexcitation γ rays of ^{92}Zr, measured at 3.20 MeV. Comments in the captions to Figs. 11 and 13 also apply to this figure.

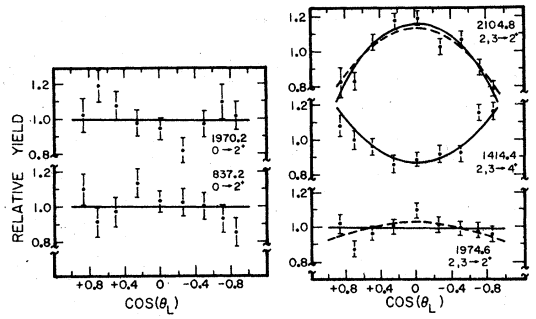

FIG. 15. Angular distributions of deexcitation γ rays of ^{92}Zr, measured at 3.70 MeV. Comments in the caption to Figs. 11 and 13 also apply to the figure.

and WHF codes written here, the magnetic substate populations of excited levels and inelastic scattering cross sections were calculated for all combinations of J^π from 0^+ to 5^-. For $J>6$ the cross sections at these energies are too small to be detected and were therefore not calculated. Theoretical γ-ray distributions, expressed as $W(\theta)=1+a^*_2(\delta)P_2(\cos\theta)+a^*_4(\delta)P_4(\cos\theta)$, were then calculated as a function of δ for each J^π and compared to the experimental distributions. The multipole mixing ratio of a γ-ray transition is defined as $\delta=\langle|L+1|\rangle/\langle|L|\rangle$, using the Rose and Brink[51] phase convention. Standard statistical criteria, again in-

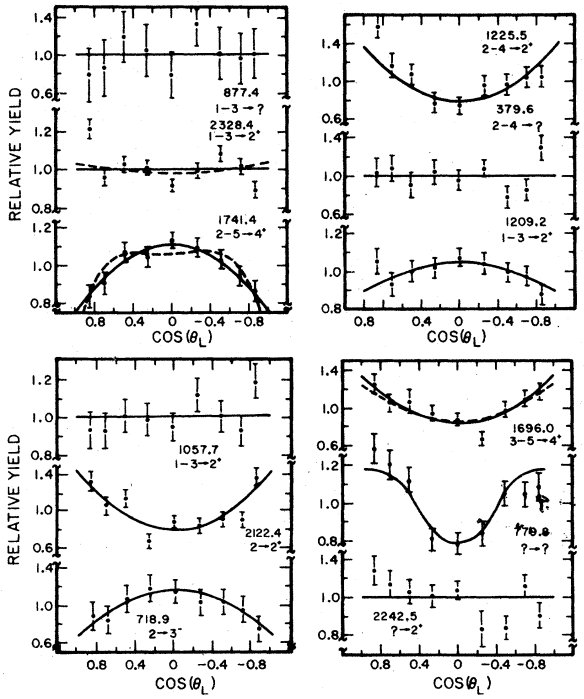

FIG. 16. Angular distribution of deexcitation γ rays of ^{92}Zr, measured at 3.70 MeV. Comments in the captions to Figs. 11 and 13 also apply to this figure.

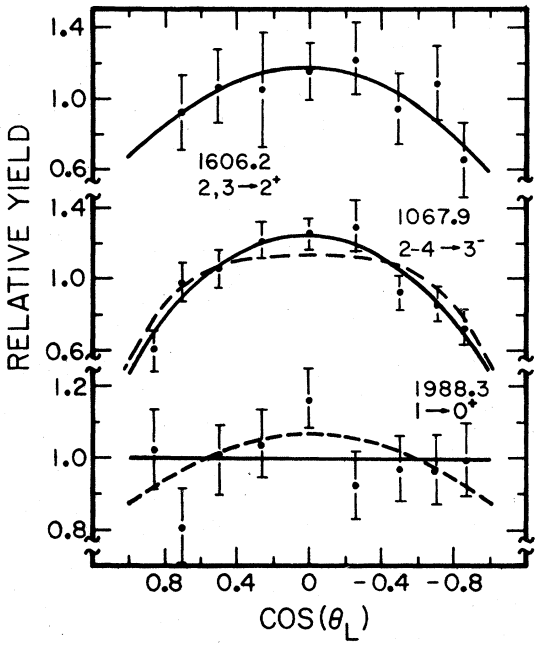

FIG. 17. Angular distributions of deexcitation γ rays of ^{92}Zr, measured at 3.70 MeV. Comments in the caption to Figs. 11 and 13 also apply to this figure.

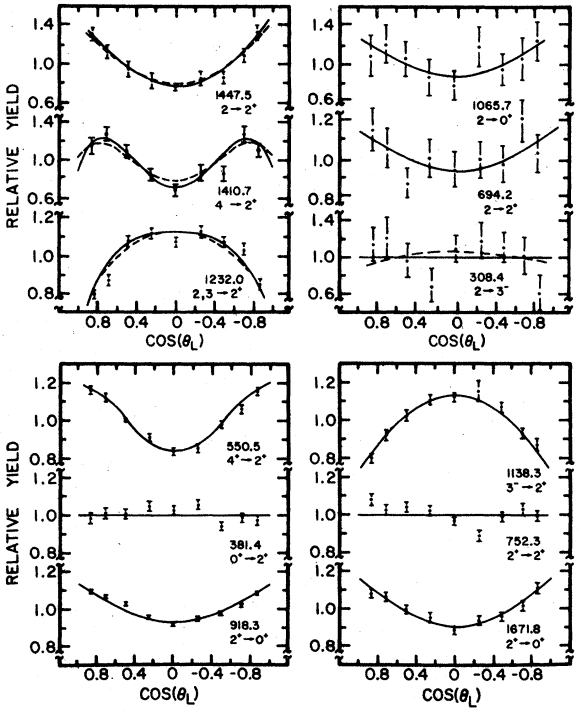

FIG. 18. Angular distributions of deexcitation γ rays of ^{94}Zr, measured at 3.10 MeV. Comments in the caption to Figs. 11 and 13 also apply to this figure.

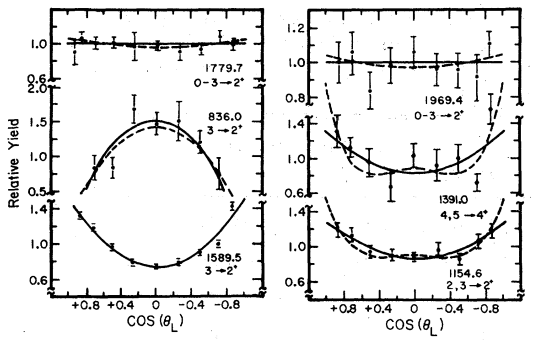

FIG. 19. Angular distributions of deexcitation γ rays of ^{94}Zr, measured at 3.10 MeV. Comments in the caption to Figs. 11 and 13 apply to this figure.

cluding the χ^2 and F_χ tests,[48] were used to determine goodness of fit. For a theoretical fit to be considered acceptable, a_2^* (or a_4^*) differed from a_2 (or a_4) by less than the experimental uncertainty given in Table III or IV. Spin discrimination was also based on the agreement of calculated and measured inelastic scattering cross sections, but only at the factor-of-2 level. That is, spin assignments which resulted in calculated cross sections differing from measured ones by more than a factor of 2 were generally rejected.

Table V summarizes the acceptable spins and the multipole mixing ratios determined from the analysis of the ^{92}Zr angular distributions and cross sections at the two bombarding energies. The values of the mixing ratios of the γ rays from the levels through the 2909.0-keV level are from the $E_n = 3.20$-MeV angular distribution results while those from the energy levels above 2909.0 keV are from the analyses of the $E_n = 3.70$-MeV measurements. Table VI lists a similar summary for ^{94}Zr. The parities given in Tables V and VI are those determined in the present study using previously known J^π values of final states and the systematics of $M2/E1$ and $M3/E2$ mixing ratios. It is generally accepted that very large admixtures of $M(L+1)$ into $E(L)$ decays do not occur. In the present work, it was assumed that mixed $L=1$ and $L=2$ transitions for which $|\delta| > 1.0$ could not be $M2/E1$. This criterion is supported by the recent compilation of $M2/E1$ mixing ratios of Beer and Arya.[52] (See Appendix B for details.) A similar criterion was used for $M3/E2$ transitions.

Tables VII and VIII compare the ^{92}Zr and ^{94}Zr neutron inelastic scattering cross sections inferred from the results of these experiments to those predicted by the WHF formalism. For the higher energy levels where a unique J^π was not determined, J^π values consistent with the experimental results were arbitrarily chosen for inclusion in this table. The level-by-level discussions to follow include the cross sections predicted for other possible spin assignments consistent with the angular distributions.

The WHF neutron inelastic scattering cross sections near threshold often are larger than the measured scattering cross sections. The theory has been modified to give a better representation of neutron scattering under these conditions.[53,54] Tessler *et al.*,[14] Glickstein *et al.*,[30] and others[54] note that at higher incident neutron energies the results of plain and modified WHF theories differ very little. The results of the present analysis support that conclusion; our calculations show that the Lane-Dresner modification causes only a 5–20% reduction in the cross sections at these energies.

The inelastic cross sections from the Lane-Dresner modification[53] of the WHF formalism are presented in Tables VII and VIII (LD was not used at 3.7 MeV). The cross sections inferred from the γ-ray measurements for the first eight levels in each of Tables VII and VIII are in good agreement with the WHF calculations. For ^{92}Zr and ^{94}Zr combined, at 3.1 and 3.2 MeV, the average magnitude of the deviation of calculated from inferred cross section is 10% for the first eight levels and 28% for all levels. In only 4 of 50 cases did spin assignments obtained from γ-ray angular distributions lead to calculated cross sections different from inferred ones by more than a factor of 2. These four cases occur at $E_n = 3.7$ MeV, where the calculated cross sections were not used to limit spin choices. At 3.1- and 3.2-MeV incident energy the sum of the calculated cross sections for all levels observed agreed with the sum of the measured ones to within $\leq 5\%$.

At 3.7-MeV incident energy, calculations were compared to measurements for ^{92}Zr. The agreement was not as good, with an average deviation magnitude of 71%. We believe this is partly because our potential was designed to represent measurements at 2.50 and 2.75 MeV and partly because the level scheme of ^{92}Zr was not well determined above 2.8-MeV excitation energy. The poorest agreement was for measurements to levels above 3-MeV excitation energy.

The question of an average potential for the description of scattering by many nuclei in the $A \simeq 90$ region is being explored in another study,[28] to be presented later. Cross sections of the WHF model were calculated also with this potential, which included an isospin term, as an additional check on the validity of the model. The calculated cross sections differed somewhat level by level from those shown in Tables VII and VIII, and showed somewhat better agreement at 3.7 MeV, but in no case was the difference large enough to have altered a spin assignment or limitation.

These results are interesting in that this is one of the few cases in which the inelastic cross sec-

TABLE V. γ-ray multipole mixing ratios and angular distribution coefficients predicted by WHF theory for the spins assigned to the levels of ^{92}Zr in this study. Parities are taken from Ref. 2 or determined from multipole mixing ratio systematics. This table shows all J^π values consistent with the present experiment (except for those with superscript c). The notation 0.36/1.92 means δ could be anywhere in the range 0.36 to 1.92.

Level (keV)	E (keV)	J^π	δ	Type	Coefficients a_2^*	a_4^*
2066.1	1132.0	2^+	1.04 ± 0.11	$M1, E2$	−0.21	−0.01
		2^+	$2.41^{+0.41}_{-0.27}$	$M1, E2$	−0.21	−0.20
		3	0.01 ± 0.01	1, 2	−0.22	0.0
2339.0	492.2	3	$-0.04^{+0.04}_{-0.00}$	1, 2	−0.19	0.0
	843.6	3	-0.13 ± 0.04	1, 2	−0.24	0.0
	1405.7	3	$0.04^{+0.00}_{-0.04}$	1, 2	−0.31	0.0
2398.0	902.6	3	0.41/1.92	1, 2	0.31	0.01
		4^+	$-1.30^{+0.30}_{-0.13}$	$M1, E2$	0.28	−0.14
		4	0.13 ± 0.09	1, 2	0.29	0.0
	1464.4	3	-0.41 ± 0.05	1, 2	0.29	0.02
		4	$0.13^{+0.05}_{-0.09}$	2, 3	0.27	−0.24
		4^-	$5.67^{+17.3}_{-1.16}$	$M2, E3$	0.25	−0.16
2485.1	990.3	5	$-0.04 + 0.00$	1, 2	−0.20	0.0
2742.6	257.3	4^-	≤ -11.4	$M1, E2$	−0.32	0.11
		4	$-0.09^{+0.05}_{-0.08}$	1, 2	−0.27	0.00
		4^-	≥ 22.9	$M1, E2$	−0.20	0.11
	403.8	4 [a]	0.00 ± 0.04	1, 2	−0.28	0.00
		4^- [a]	$7.6^{+15.3}_{-3.1}$	$M1, E2$	−0.19	0.33
		4 [b]	$0.04^{+0.13}_{-0.04}$	1, 2	−0.33	0.00
		4^- [b]	$5.7^{+17.2}_{-1.2}$	$M1, E2$	−0.24	0.27
	1248.0	4	0.13 ± 0.04	1, 2	0.31	−0.06
2818.0	972.0	2	0.18 ± 0.04	1, 2	0.11	0.0
		2^+	$-4.51^{+0.78}_{-1.16}$	$M1, E2$	0.09	−0.03
		3	$-0.27^{+0.05}_{-0.00}$	1, 2	0.13	0.01
	1883.6	2	$0.22^{+0.09}_{-0.05}$	1, 2	0.08	0.0
		2^+	≤ -3.73	$M1, E2$	0.06	−0.03
		3	-0.22 ± 0.04	1, 2	0.06	0.0
2863.6	1369.3	3	0.18 ± 0.04	1, 2	0.08	0.0
		4	0.47 ± 0.05	1, 2	0.05	−0.05
		5	$-0.18^{+0.00}_{-0.05}$	1, 2	0.03	0.01
	1928.7	3	−3.73/−0.58	1, 2	0.66	0.09
		4	$-0.32^{+0.28}_{-0.19}$	2, 3	0.69	0.12
		4^-	≤ -3.73	$M2, E3$	0.67	0.20
		5	$0.00^{+0.18}_{-0.09}$	3, 4	0.72	0.08
2903.8	837.2	0		2	0.0	0.0
	1970.2	0		2	0.0	0.0
2909.0	1414.4	2	$0.52^{+0.57}_{-0.34}$	2, 3	0.27	0.0

TABLE V. *(Continued)*.

Level (keV)	E (keV)	J^π	δ	Type	Coefficients a_2^*	a_4^*
		3	$0.41^{+0.17}_{-0.10}$	1, 2	0.28	0.0
		3^+	$1.73^{+0.68}_{-0.43}$	$M1, E2$	0.29	0.03
	1974.6	2	0.47 ± 0.05	1, 2	−0.09	0.0
		2^+	$\sim\infty$	$M1, E2$	−0.11	−0.03
		3	$-0.13^{+0.04}_{-0.00}$	1, 2	−0.08	0.0
3038.9	2104.8	2^+	$1.57^{+0.84}_{-0.48}$	$M1, E2$	−0.28	−0.02
		3	$0.04^{+0.09}_{-0.04}$	1, 2	−0.33	0.0
3056.5	718.9	2	$-0.41^{+0.14}_{-0.17}$	1, 2	−0.29	0.0
		2^-	$-4.51^{+1.76}_{-3.09}$	$M1, E2$	−0.29	0.01
		3^- [c]	1.00 / 7.60	$M1, E2$	−0.31	−0.07
	2122.4	2	$-0.41^{+0.28}_{-1.16}$	1, 2	0.41	0.0
		3^+ [c]	$-3.17^{+0.76}_{-4.42}$	$M1, E2$	0.48	0.16
3124.4	1057.7	1	≥ -0.32	1, 2	0.024	0.0
		2	$0.32^{+0.21}_{-0.14}$	1, 2	0.01	0.0
		3	$-0.18^{+0.04}_{-0.09}$	1, 2	−0.01	0.01
3190.8	1696.0	3	0.41 / 1.92	1, 2	0.36	0.03
		4	0.09 ± 0.13	1, 2	0.34	0.0
		4^+	$-1.30^{+0.46}_{-0.27}$	$M1, E2$	0.29	−0.16
		5	-0.36 ± 0.05	1, 2	0.33	0.05
3236.2	1741.4	2	$-0.70^{+0.06}_{-0.07}$	2, 3	−0.25	0.0
		3	$-0.13^{+0.04}_{-0.01}$	1, 2	−0.26	0.0
		3^+	$\sim\pm\infty$	$M1, E2$	−0.19	0.04
		4^+	$1.09^{+0.10}_{-0.09}$	$M1, E2$	−0.25	−0.14
		5	$-0.04^{+0.04}_{-0.00}$	1, 2	−0.20	0.0
3262.2	2328.4	1	$1.19^{+0.95}_{-1.11}$	1, 2	0.04	0.0
		2	$0.27^{+0.05}_{-0.09}$	1, 2	0.04	0.0
		3	-0.22 ± 0.04	1, 2	0.06	0.01
3275.9	1209.2	1	≤ -0.27	1, 2	−0.10	0.0
		2	$0.52^{+0.08}_{-0.11}$	1, 2	−0.12	−0.01
		2^+	$\sim\infty$	$M1, E2$	−0.10	−0.03
		3	$-0.13^{+0.04}_{-0.00}$	1, 2	−0.08	0.0
3288.7	1225.5	2	−1.92/−0.04	1, 2	0.41	−0.02
		3	$-0.52^{+0.16}_{-0.12}$	1, 2	0.43	0.04
		4	0.00 ± 0.13	2, 3	0.41	−0.16
		4^-	≤ -11.4	$M2, E3$	0.47	0.0
		4^-	≥ 7.6	$M2, E3$	0.39	0.0
3370.9	1988.3	1		1	−0.13	0.0
3407.9	1067.9	2^-	$-1.19^{+0.49}_{-0.73}$	$M1, E2$	−0.47	0.0
		3^-	$1.73^{+2.80}_{-0.73}$	$M1, E2$	−0.36	−0.11
		4	0.13 ± 0.04	1, 2	−0.51	0.0

TABLE V. *(Continued).*

Level (keV)	E (keV)	J^π	δ	Type	Coefficients a_2^*	a_4^*
3452.2	1606.2	2^+	$1.57^{+1.18}_{-0.57}$	$M1,E2$	−0.31	−0.02
		3	$0.04^{+0.09}_{-0.04}$	1, 2	−0.36	0.0

[a] WHF fit to data taken at $E_n = 3.2$ MeV.
[b] WHF fit to data taken at $E_n = 3.7$ MeV.
[c] Since the parities of the $J=3$ fits to these γ rays are mutually exclusive, $J=3$ is eliminated for this level.

tions to very many levels have been measured and then analyzed with potentials obtained from elastic scattering data in the same mass and energy regions.

^{92}Zr angular distributions

Figure 11 shows the angular distributions of γ rays from the first five excited levels of ^{92}Zr. These distributions have the shapes expected for the known J^π values involved. γ rays from these energy levels are strong and their distributions are well fitted by even-order Legendre polynomial expansions.

2066.1-keV. Several studies[2] have narrowed choices for this level to $J=1$ or 2. A (t,p) study[3] clearly establishes 2^+ for this level, excited as an $l=2$ transfer from the 0^+ ground state of ^{90}Zr. Both the angular distribution presented here for the 1132-keV decay and the inelastic scattering cross sections are consistent only with $J=2$ or 3, and thus support the 2^+ assignment of Ref. 3.

2339.0-keV. The angular distributions of all three decays from this known 3^- level are in agreement with the WHF calculations as shown in Fig. 12, but our measured branching ratios disagree with those previously reported.[55] Our relative intensities for the 492.2- and 1405.7-keV γ rays agree well with those of Ref. 55, but the yields for the 843.6-keV line were difficult to extract from the shoulder of the 847-keV background line. and this may have led to error in our intensity measurement for that line.

2398.0-keV. The WHF fits to the 902.6- and 1464.4-keV distribution limit the possible spin assignments of the 2398.0-keV level to either 3 or 4. The inferred 98 ± 9 mb cross section agrees better with 109 mb predicted by WHF calculations for $J^\pi = 4^+$ than with the 152 mb predicted for $J^\pi = 3^+$. While this supports the 4^+ assigned to this level from the results of (d,p) studies,[5] $J=3$ cannot be rejected by the present experiment. At 3.20 MeV $J=4$ gives the dashed curves shown with both angular distributions in Fig. 12.

2485.1-keV. While a 5^- assignment had tentatively been made for this level,[4,8,9] the recent capture study of Fanger *et al.*[11] reported a decay from it

TABLE VI. γ-ray multipole mixing ratios and angular distribution coefficients predicted by WHF theory for the spins assigned to the levels of ^{94}Zr from this study.

Level (keV)	E (keV)	J^π	δ	Type	Coefficients a_2^*	a_4^*
2150.3	1232.0	2^+	$1.73^{+1.44}_{-0.82}$	$M1,E2$	−0.25	−0.02
		3	0.00 ± 0.04	1, 2	−0.24	0.0
2329.0	1410.7	4	$0.13^{+0.09}_{-0.13}$	2, 3	0.27	−0.24
		4^-	$5.7\ ^{+17.2}_{-1.2}$	$M2,E3$	0.25	−0.16
		5	$1.30^{+0.43}_{-0.60}$	3, 4	0.36	−0.40
2365.4	308.4	2	$-0.04^{+0.27}_{-0.22}$	1, 2	−0.09	0.0
		2^-	$7.60^{+\infty}_{-5.46}$	$M1,E2$	−0.08	0.0
	694.2	2	$0.09^{+0.13}_{-0.09}$	1, 2	0.16	0.0
		2^+	$-3.17^{+1.03}_{-1.34}$	$M1,E2$	0.14	−0.02
	1065.7	2	0	2	0.30	−0.09
	1447.5	2	$-0.64^{+0.12}_{-0.14}$	1, 2	0.42	−0.01
2507.6	836.0	3	$0.84^{+0.46}_{-0.43}$	1, 2	−0.84	0.07
	1589.5	3	$-0.70^{+0.12}_{-0.08}$	1, 2	0.54	0.06
		3^+	$-2.14^{+0.22}_{-1.02}$	$M1,E2$	0.59	0.14
2698.0	1779.7	0^+		$E2$	0.0	0.0
		1	$0.77^{+0.65}_{-0.44}$	1, 2	0.05	0.0
		2	0.22 ± 0.05	1, 2	0.07	0.00
		2^+	$-5.67^{+2.06}_{-1.92}$	$M1,E2$	0.05	−0.03
		3	$-0.22^{+0.03}_{-0.05}$	1, 2	0.06	0.01
2825.2	1154.6	2	$-0.04^{+0.04}_{-0.13}$	1, 2	0.26	0.0
		2^+	$-1.92^{+0.35}_{-0.49}$	$M1,E2$	0.28	−0.02
		3	−0.36 ± 0.05	1, 2	0.26	0.02
		3^+	$-5.67^{+1.16}_{-1.92}$	$M1,E2$	0.35	0.19
2859.8	1391.0	4	$0.13^{+0.23}_{-0.40}$	1, 2	0.32	−0.01
		5	$-0.41^{+0.19}_{-0.11}$	1, 2	0.40	0.06
		5^+	$-3.17^{+1.60}_{-2.50}$	$M1,E2$	0.50	0.38
2887.7	1969.4	0^+		$E2$	0.0	0.0
		1	$0.77^{+1.15}_{-0.59}$	1, 2	0.05	0.0
		2	$0.22^{+0.10}_{-0.04}$	1, 2	0.08	0.00
		3	$-0.22^{+0.04}_{-0.05}$	1, 2	0.06	0.01

TABLE VII. A comparison of inferred ^{92}Zr neutron inelastic scattering cross sections to those calculated, for some selected spins, from WHF and Lane-Dresner (LD) modified WHF theory.[a]

		Neutron inelastic scattering cross sections, in mb			
		3.20 MeV		3.70 MeV	
Level (keV)	J^π	Inferred	WHF (LD)	Inferred	WHF Plain
934.1	2^+	472 ± 59	357	333 ± 48	243
1381.9	0^+	101 ± 10	99	74 ± 8	71
1494.8	4^+	144 ± 21	193	89 ± 18	138
1846.4	2^+	232 ± 23	257	145 ± 16	187
2066.1	2^+	229 ± 22	233	132 ± 17	172
2339.0	3^-	140 ± 16	129	105 ± 14	122
2398.0	4^+	98 ± 9	109	66 ± 7	87
2485.1	5^-	30 ± 10	30	34 ± 11	39
2742.6	4^-	31 ± 3	50	25 ± 3	62
2818.0	3^+	99 ± 9	74	69 ± 7	90
2863.6	4^+	37 ± 4	25	37 ± 4	29
2903.8	0^+	30 ± 5[b]	34	30 ± 3	39
2909.0	3^+	45 ± 4	79	45 ± 5	94
3038.9	3^+	12 ± 2	37[c]	26 ± 7	83
3056.5	2^-	18 ± 5[b]	40[c]	54 ± 10	98
3124.4	1^+			17 ± 2[b]	76
3177.2	4^+			30 ± 3	45
3190.8	5^+			14 ± 2	20
3236.2	4^+			24 ± 3	40
3262.2	1^+			32 ± 3[b]	62
3275.9	3^+			31 ± 3[b]	59
3288.7	4^+			26 ± 2[b]	36
3370.9	1^+			14 ± 2[b]	46[c]
3407.9	3^-			17 ± 2[b]	37[c]
3452.2	2^+			8 ± 1[b]	41[c]

[a] For WHF calculations, $\pi = +$ is assumed if π is unknown.

[b] Includes $4\pi\sigma_\gamma(90°)$ estimate for cross section of a γ ray whose angular distribution was not measured.

[c] Levels too close to threshold to be included in statistical model comparisons.

to an excited 0^+ level, which would clearly rule out the above assignment. We have looked carefully for this reported 1103.4-keV γ ray to the second 0^+ level and find no such decay. If the level were 2^+, suggested[11] because it appeared to decay both to 0^+ and 4^+ levels, such a line should have been clearly visible in our spectra because neutron scattering from even-A nuclei excites 2^+ levels strongly. The predicted WHF cross sections at $E_n = 3.20$ MeV for $J = 2$, 3, or 4 are all in excess of 81 mb, more than a factor of 2 larger than the measured 30 ± 10 mb. The 30 mb predicted for 5^- is nicely consistent with the measurement and confirms the spin assignment originally made by others. This level decays entirely to the 4^+ level.

2742.6-keV. Fanger *et al.*[11] tentatively assigned 3^+ or 4^+ to this level, but more recently Chestnut *et al.*[56] saw this level as an $l = 1$ transfer in the ^{93}Nb(d, ^{3}He)^{92}Zr reaction, and suggested it was the 4^- member od the 5^-, 4^- doublet which results from excitation of a proton from the $p_{1/2}$ subshell into the $g_{9/2}$ shell. Their ^{3}He angular distributions are not sensitive to spin, but if they treated the 2485.1- and 2742.6-keV levels as members of the ($p_{1/2}$, $g_{9/2}$) doublet with spins 5^- and 4^- respectively, the two levels exhausted the $p_{1/2}$ pickup strength. Three angular distributions of γ-ray transitions from this level are shown in the lower panel of Fig. 13 and can be fitted only with spin of 2, 3, or 4 assigned to the 2742.6-keV level. However, cross section comparisons eliminate the $J = 2, 3$ possibilities. Since the $l = 1$ transfer of Ref. 56 implies negative parity for this level, the level is uniquely determined to be 4^-. The angular distributions of the 257.3-keV transition in Fig. 13 are consistent with a dipole transition, which would be the $M1$ spin-flip transition between the two odd-parity levels, and the 1248-keV line is an $E1$ transition.

2818.0-keV. The angular distributions of the 972.0- and 1883.6-keV transitions as well as the inferred cross section agree with both $J = 2$ and $J = 3$. The decay to the ground state observed by Talbert *et al.*[6] implies $J = 1$, 2, or 3, so that $J = 2$ or 3 are the possible assignments.

2903.8-keV. Although the isotropic angular distributions of the 837.2- and 1970.2-keV transitions can both be fitted for $J = 0$–3, the calculated WHF cross sections exceed 69 mb for $J = 1$–3. Hence, $J = 0$ can be assigned to the 2903.8-keV level on the basis of cross section magnitude.

3056.5-keV. The WHF cross sections agree with experiment for $J = 2$ and $J = 3$, but since the parities for the $J = 3$ fits to the 718.9- and 2122.4-keV angular distributions are mutually exclusive, $J = 3$ is eliminated. On the basis of the fits to these two transitions, the 3056.5-keV level has $J = 2$. This is probably the 2^+ level seen in several particle transfer and inelastic scattering experiments.[3,5,10]

3370.9-keV. Although the WHF cross sections for $J = 1$, 4, and 5 agree with the data, only the WHF angular distribution for $J = 1$ agrees with the observed isotropic angular distribution to a 0^+ final state. Also $J = 4$, 5 are not allowed by the log ft value measured[6] in the β decay to this level. Hence, the experiments imply a unique $J = 1$ spin assignment.

For the three levels, at 2909.0, 3038.9, and 3452.2 keV, analysis of angular distributions of deexcitation γ rays limits the possible spin assignments to $J = 2$ or 3. It should be noted, however, that for one of these, the 3038.9-keV level, the comparison of inferred and WHF cross sections is inconsistent with either assignment. This is the only case of a failure of the cross section test of

TABLE VIII. A comparison of inferred and calculated ^{94}Zr neutron inelastic scattering cross sections for E_n = 3.10 MeV, and some selected spins. Calculated cross sections were obtained using WHF theory modified to include Lane-Dresner width-fluctuation corrections. [a]

Level (keV)	J^π	Neutron inelastic scattering cross section, in mb Inferred	WHF (LD)
918.3	2^+	385 ± 51	318
1299.7	0^+	90 ± 10	87
1468.8	4^+	183 ± 18	177
1671.2	2^+	247 ± 25	240
2056.6	3^-	169 ± 16	150
2150.3	2^+	190 ± 18	190
2329.0	4^+	84 ± 9	103
2365.4	2^+	190 ± 18	165
2507.6	3^+	112 ± 11	124
2603.7 [b]	5^-	25 ± 8	24
2698.0	0^+	53 ± 5	38
2825.2	3^+	56 ± 5	62
2846.0 [b]	1^+	35 ± 10	57
2859.8	4^-	22 ± 3	32
2887.7	0^+	27 ± 3	22

[a] For WHF calculations, $\pi = +$ is assumed if π is unknown.

[b] Inferred cross section is estimated from 90° excitation function using $\sigma_{inf} = 4\pi\sigma_\gamma(90°)$, which assumes an isotropic angular distribution.

spin assignments in either ^{92}Zr or ^{94}Zr at 3.2 or 3.1 MeV, where the inferred cross sections are well enough determined to limit spin choices, and it occurs very close to threshold for excitation of the level. The WHF model, even as modified by fluctuation corrections,[53] is not reliable near threshold.

Analyses of the data for the weakly excited levels above 3.1-MeV excitation energy provide less information. For all of the levels observed $J \leq 5$, and for most of them more stringent limits can be placed, as indicated in Table V and Fig. 1. Detailed discussions of the analyses for each of the levels and all of the γ-ray angular distributions are given in the dissertation of one of the authors.[57]

In Figs. 11–15 and Table III, the ^{92}Zr angular distributions, coefficients of least-squares fits to the data, and γ-ray intensities are compared for the measurements at 3.20- and 3.70-MeV incident energy. The a_2 coefficients change little with the 0.5-MeV increase in bombarding energy, and the branching ratios for decay of the levels are in excellent agreement as extracted from data at the two incident energies.

^{94}Zr angular distributions

The angular distributions of the γ rays from the ^{94}Zr levels for which the spin-parities were known prior to this study have the characteristics generally expected for the J^π values involved. The experimental and calculated cross sections are given in Table VIII. The Lane-Dresner correction,[53] previously discussed, was used even though it is smaller than the experimental uncertainties at 3.10 MeV.

2150.3-keV. A 2^+ has previously been assigned[4,13] to the 2150.3-keV level. The distributions predicted by the WHF theory for $J = 2$ and 3 coincide, as indicated by the single dashed curve shown with the 1232.0-keV γ-ray angular distribution in Fig. 18. The WHF inelastic scattering cross section for $J^\pi = 2^+$, 190 mb, agrees with the inferred value of 190 ± 18 mb.

2329.0-keV. The resolution of confusion surrounding the report of levels near this excitation energy was one of the first results of this $(n, n'\gamma)$ study.[1] Two levels were discovered, both emitting γ rays near 1.4 MeV. Although earlier studies of the β decay of ^{94}Y failed to report both levels,[17,18,58] a recent reexamination of that decay also provides evidence for both of them.[19]

The 1410.7-keV γ ray to the first 2^+ level, shown in Fig. 4, includes a weak, forward peaked, background component, estimated at ~5%. The angular distribution of the combined yields was not symmetric about 90°, but with care the background was subtracted, leaving a symmetric angular distribution for the 1410.7-keV γ ray. The fits to the background-subtracted data are given in Tables IV and VI. Only theoretical distributions for $J = 4$, 5 fit the background-subtracted data. The WHF calculated cross section for $J = 5$ differs by a factor of 1.7 from the inferred 84 mb; furthermore, an $L = 3$ or $L = 4$ decay as the sole decay of a $J = 5$ level would be highly improbable. Also, when the 886.2-keV γ ray is correctly placed in the decay scheme, so that it is not feeding the 2329.0-keV level, the log ft value for β decay[19] to the level becomes 9.0, and this eliminates $J^\pi = 4^-$, $5^\pm$ for this level according to the rules of Raman and Gove.[59] The predicted 103 mb for $J = 4$ agrees within the accuracy of the statistical model with the inferred 84 mb, and hence $J^\pi = 4^+$ is the unique assignment established by the combined experiments.

2365.4-keV. This is the other level in this region of excitation decaying by a γ ray near 1.4 MeV, as well as by other transitions. Although the 308.4-, 694.2-, and 1447.5-keV γ-ray angular distributions can be fitted with both $J = 2$ and $J = 3$, the angular distribution of the 1065.7-keV γ ray to a 0^+ final state only agrees with $J = 2$. The large mixing ratio of the 1447.5-keV fit implies $J^\pi = 2^+$, in good agreement with earlier work. The questions raised by Tessler *et al.*[14] are resolved since the $J^\pi = 4^+$ level at 2329.0-keV and the $J^\pi = 2^+$ level

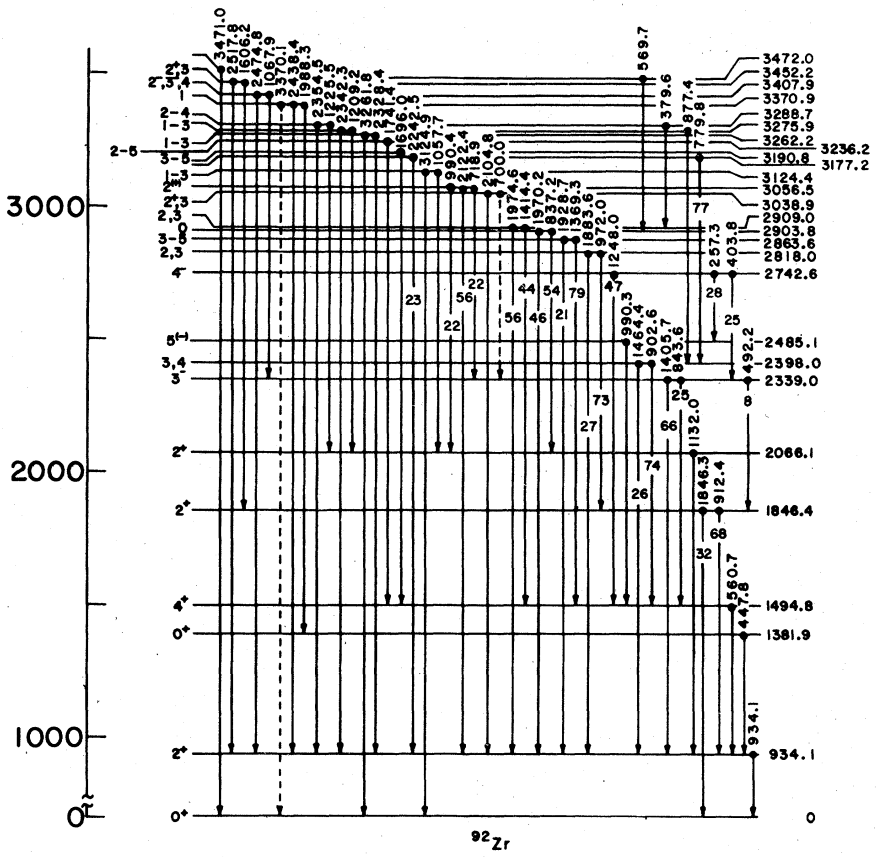

FIG. 20. The level scheme of ^{92}Zr. The level energies and γ-ray energies in keV and the branching ratios are those determined in this study. The spins and parities above 2.3 MeV were mostly determined in this study. A notation such as 2–4 indicates the possible spin assignments to the level are limited to 2, 3, or 4.

at 2365.4 keV are both excited in the present $(n,n'\gamma)$ reaction study.

2507.6-keV. The 2507.6-keV level, discovered in this experiment, emits 836.0-keV and 1589.5-keV γ rays, both of which decay to 2^+ levels. While distributions for $J=2$, 3, 4, and 5 fit the measured 1589.5-keV distribution, the exceptionally strong negative anisotropy of the 836.0-keV distribution is predicted only for $J=3$. Since the multipole mixing ratios for $J=3$ are all quite large[52] for an $M2$-$E1$ mixture, the parity is probably positive. The cross section magnitude comparison also confirms our $J=3$ assignment.

2603.7-keV. No angular distribution was obtained for the 1134.9-keV γ ray from the 2603.7-keV level known[4] to be 5^-, but the calculated and measured cross sections agree only for that assignment, assuming a reasonable anisotropy for the $E1$ decay to the 4^+ level. The reported $J^\pi=5^-$ of Ref. 4 is thus confirmed.

2698.0-keV. Predicted angular distributions for spins 0 through 3 all can be nearly isotropic and fit the isotropic distribution measured for the 1779.7-keV γ ray from the 2698.0-keV level. The WHF inelastic scattering cross sections for all of these spins are consistent with the inferred 53 mb, so the spin of this level is $J\leq 3$.

2825.2-keV. The least-squares fit to the angular distribution of the 1154.6-keV γ ray from the 2825.2-keV level coincides with the distributions predicted for $J=2$ and 3. The WHF inelastic cross sections for $J=2$ and 3 both agree with the measured value and the spin assignment to the level is limited to these two spins.

2846.0-keV. No angular distribution was obtained for the transition to the ground state, but the inelastic cross section was estimated from the excitation function. The fact that this level is seen [17,19,58] following β decay from ^{94}Y with log $f_0t=7.8$ and log $f_1t=8.9$ limits its spin to 0^+, 1–3, 4^+; the fact that it decays directly to the ground state certainly eliminates 0^+, 3^+, and 4^+ and probably eliminates 3^- as a possibility. The calculated cross sections for spins 1 and 2 are consistent

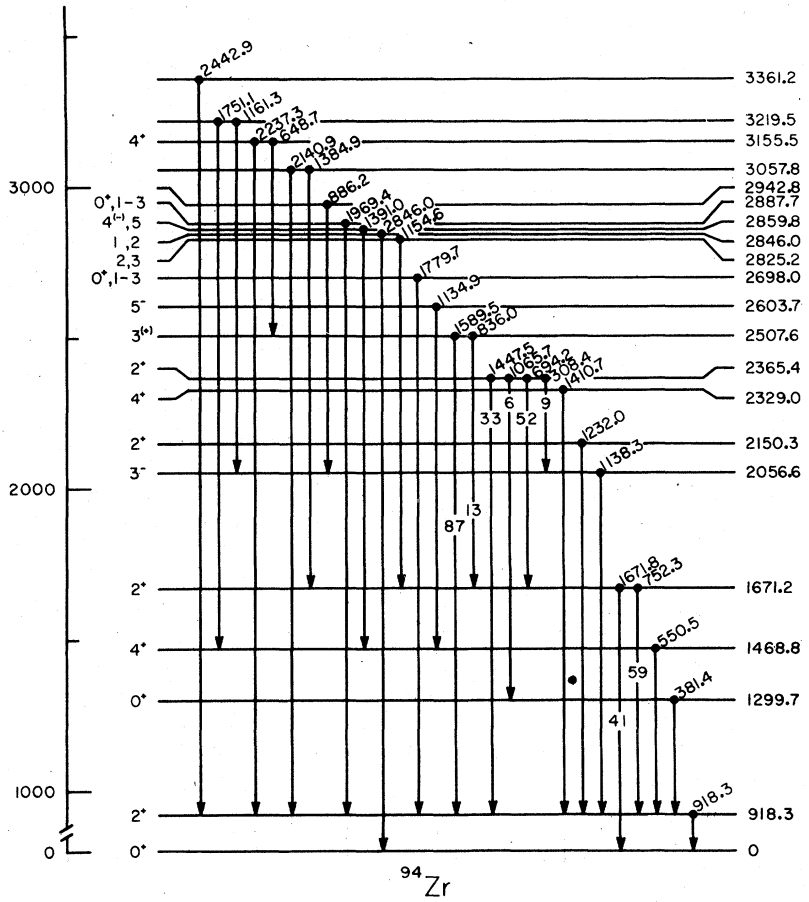

FIG. 21. The level scheme of ^{94}Zr. The level energies and γ-ray energies in keV and the branching ratios are those determined in this study. The spins and parities above 2.2 MeV were mostly determined in this study. The notation 0–3 indicates the possible spin assignments to the level are 0, 1, 2, or 3.

with the measured value, especially when the 10% branching[19] to the first excited state is included. Thus, we can limit the spin of this state to $J=1$ or 2.

2859.8-keV. The 1391.0-keV γ ray angular distribution has a large anisotropy which can be fitted only with $J=4$ or 5. If it is 4^-, then the 1391.0-keV decay is the $4^- \rightarrow 4^+$ $E1$ decay analogous to the 1248.0-keV γ-ray deexciting the 4^- level at 2742.6 keV in ^{92}Zr. A search on the mixing ratio δ for $J=4$ gives the expected result, that $|\delta| \lesssim 0.2$ so the decay would be close to pure $E1$, as in ^{92}Zr.

Our results suggest that the 2859.8-keV level is the 4^- member of the 5^-, 4^- doublet corresponding to excitation of a proton from the $p_{1/2}$ to the $g_{9/2}$ shell. On this basis, we looked for the $M1$ transition of 256.1 keV between the levels. The corresponding 257-keV transition in ^{92}Zr is quite strong, but no sign of the 256.1-keV transition exists in the ^{94}Zr data.

One can ask whether other candidates for the expected 4^- level exist. Between 2.7- and 3.2-MeV excitation energy all other levels except that at 2846.0 keV either decay directly to 2^+ levels or are strongly excited in the (t,p) reaction,[3] or both. The 2846.0-keV level cannot be $J^\pi=4^-$ because of its ground-state decay, β-decay feeding, and inferred cross section size. The 5^- levels are seen to be very weakly excited in the two-neutron transfer studies,[3,4] and the 4^- levels are not visible at all, which is consistent with the fact that they are proton excitations. Since it appears that the only candidate for the 4^- level in ^{94}Zr is this new level discovered at 2859.8 keV, the 4^- assignment is strongly favored.

2887.7-keV. Based on the 1969.4-keV angular distribution, spins 4 and 5 are definitely rejected for the 2887.7-keV level. No further limitation on the acceptable spins 0 through 3 has been determined. With the exception of $J=0$, the acceptable spins yield the dashed curve shown with the distribution.

The final descriptive level schemes, shown in

Figs. 20 and 21 summarize for ^{92}Zr and ^{94}Zr the level energies, γ-ray energies, and branching ratios determined in this study. The spin assignments and limitations for levels above 2.3 MeV are recommended values and are based on the evidence from this study, in a few cases combined with evidence from other studies. The parities are those adopted by Refs. 2 and 13, or were determined in the present work using multipole mixing ratio systematics.[52]

^{92}Zr neutron inelastic scattering cross sections

As noted in the Introduction, the neutron inelastic scattering cross sections $\sigma_{n'}$ inferred from the results of the $(n,n'\gamma)$ experiments can be compared to those measured directly in (n,n') experiments.[32] These two types of neutron experiments normally have different objectives and usually are not undertaken at the same incident neutron energies. However, in the case of ^{92}Zr the data of Guenther *et al.*[31] include measurements at 3.2 MeV which can be compared directly to the present results at 3.20 MeV. This comparison is shown in Table IX. In all cases, the discrepancies are within the combined errors on the two measurements, each measurement having an uncertainty of about 10%. This good agreement of results measured with different methods in different laboratories is quite encouraging, and lends confidence to the use of the compilation of measurements[44,45] of the 847-keV γ-ray production cross sections in ^{56}Fe as a standard for $(n,n'\gamma)$ measurements. This compilation is, of course, useful only for incident neutron energies from 2.0 to 5.0 MeV, and for measurements made using a sufficiently large incident neutron energy spread.

For cross section comparisons at incident neutron energies other than those where the $(n,n'\gamma)$ angular distributions were measured, the $(n,n'\gamma)$ excitation functions can be used to extrapolate the angle-integrated γ-ray production cross sections σ_γ to the proper energy so that the inelastic neutron cross sections can be inferred and compared to the directly measured values. In order that the comparison be valid, certain criteria must be satisfied. The range of the extrapolation should not be too large because the anisotropies of the γ-ray angular distributions can change if the number of cascades feeding the decaying level changes. All γ rays cascading to and emitted from a level must be identified and their angle-integrated cross sections accurately measured. Failure to include even one strong γ ray or several weak ones can introduce serious error. Based on excitation function data, $4\pi\sigma_\gamma(90°)$ often can be used as an estimate of the angle-integrated cross section of a γ ray for which an angular distribution was not obtained. However, this approximation introduces additional uncertainties into the inferred neutron inelastic scattering cross sections. Careful sample-size corrections must be made to the data from the (n,n') and $(n,n'\gamma)$ experiments.

The angle-integrated γ-ray production cross sections obtained from the ^{92}Zr 3.20-MeV angular distribution experiment satisfy these criteria and have been extrapolated to 2.75 MeV. Table IX compares the inelastic neutron scattering cross sections inferred from these results to those measured directly from (n,n') experiments carried out both in this laboratory[28] and at ANL.[31] (The ANL values were obtained by interpolation on their Fig. 5.) The agreement at 2.75 MeV is worse than at 3.20 MeV, probably due to the additional errors added by the extrapolation. The difference at 2.75 MeV between the directly measured[28] and inferred cross sections for the levels at 1846.4 keV and 2066.1 keV probably results from insufficient resolution to properly separate the two neutron groups. The sum of the measured cross sections for these two levels does agree with the sum of inferred values from this study. This is an example of the

TABLE IX. A comparison of neutron inelastic scattering cross sections in ^{92}Zr from (n,n') and $(n,n'\gamma)$ measurements. A direct comparison of complete γ-ray measurements and n-detection results is given at 3.2 MeV. The 90° γ-ray excitation functions were used to extrapolate the γ-ray results to other energies where n-detection data were available, 2.75 and 3.5 MeV.

	2.75 MeV			3.20 MeV		3.50 MeV		
Level energy	$(n,n'\gamma)$	Ref. 28 (n,n')	Ref. 31 (n,n')	$(n,n'\gamma)$	Ref. 31 (n,n')	$(n,n'\gamma)$	Ref. 60 (n,n')	Ref. 31 (n,n')
934.1	633	606	535	472	385	421	283	315
1381.9	108	109	140	101	115	84	58	80
1494.8	183	254	245	144	175	130	153	160
1846.4	240	340	320	232	250	192	172	220
2066.1	240	160	275	229	235	181	157	150
2339.0				140	165	126	{234}	130
2398.0				98	120	89		105

situation mentioned in the Introduction, in which for closely spaced levels, the high resolution $(n,n'\gamma)$ method can give more precise values for inelastic neutron scattering cross sections than direct measurement via neutron detection.

At 3.50 MeV the criteria mentioned above for reliable extrapolation of the $(n,n'\gamma)$ data are not all satisfied. Above 3.0-MeV excitation energy in ^{92}Zr there are many levels, and weak decays from these levels are poorly defined by our measurements. A special problem exists for the 990.3-keV line, as it becomes a composite 990.3–990.4-keV line with possible changes in its angular distribution, and other angular distributions may also change. Nonetheless, since our $(n,n'\gamma)$ excitation function data extend to 3.70 MeV, we used them to construct a comparison at 3.50 MeV where neutron detection results[31,60] exist. With the exception of the 934-keV level, the agreement is surprisingly good, especially considering the possible sources of error. The discrepancy for the first excited state is understandable since it is fed by many weak cascades from higher levels. The expected changes in γ-ray angular distributions are also in a direction to cause overestimation of the 2^+ cross section.

V. SUMMARY

A spectroscopic study of the γ radiations following the inelastic scattering of neutrons with energies from 2.22 to 3.70 MeV from nearly pure isotopic samples of ^{92}Zr and ^{94}Zr has been made to improve our knowledge of the level structure of these two nuclei and to determine the neutron inelastic scattering cross sections for the various excited levels. Cross sections for such closely spaced levels could not have been obtained easily by any other technique. Measurements of 90° γ-ray production cross sections with good γ-ray energy resolution at 50-keV neutron energy increments properly placed the γ rays, including many weak transitions, in the isotope decay schemes, and determined the level energies to within 1 keV. The agreement of many of the γ-ray energies, 90° production cross sections, level branching ratios, and level energies measured in this study with previously reported values of these quantities justifies confidence in those values that are reported here for the first time.

The ^{92}Zr excitation function identified 51 γ rays, several of which were previously unreported, from 26 levels up to 3472.0 keV. Two new levels, at 2903.8 and 3407.9 keV, were discovered. Our measured level energies agree best with those reported by Fanger *et al.*[11] and this agreement has helped us to clarify the level structure of ^{92}Zr. For ^{92}Zr we have measured 24 angular distributions of γ rays from levels through 3056.5-keV excitation energy at 3.20-MeV incident neutron energy and 39 angular distributions for transitions from levels through 3452.2 keV at 3.70-MeV neutron energy. The analyses of these angular distributions resulted in the unique or limiting spin and parity assignments given in Table V and in Fig. 1. Based on our own results, we have made unique assignments to the following six levels in ^{92}Zr (E_X in keV, J^π); 2339.0, 3; 2485.1, 5; 2742.6, 4; 2903.8, 0; 3056.5, 2; 3370.9, 1. For the first six excited levels, with previously determined spin and parity assignments, the γ-ray angular distributions calculated within the WHF model agreed very well with those measured, confirming once again the validity of using such distributions for spectroscopy. For all higher levels, previous work had left the assignments in doubt or completely undetermined. When this experiment is combined with the work of others, the following assignments or limitations are arrived at (level energies in keV followed by acceptable J^π assignments): 2398.0, 3, 4; 2485.1, $5^{(-)}$; 2742.6, 4^-; 2818.0, 2, 3; 2863.6, 3–5; 2903.8, 0; 2909.0, 2, 3; 3038.9, 2^+, 3; 3056.5, $2^{(+)}$; 3124.4, 1–3; 3190.8, 3–5; 3236.2, 2, 3, 4^+, 5; 3262.2, 1–3; 3275.9, 1–3; 3288.7, 2–4; 3370.9, 1; 3407.9, 2^-, 3^-, 4; and 3452.2, 2^+, 3. γ-ray branching ratios were measured and the γ-ray multipole mixing ratios were obtained for the indicated spin possibilities.

The ^{94}Zr excitation studies identified 28 γ rays, 12 of which were formerly unidentified, from 20 levels up to 3361.2 keV. A previously reported ambiguity concerning 2^+ and 4^+ levels in the 2320- to 2365-keV energy region has been resolved. We have shown that there are, in fact, two γ-decaying levels in this energy region, a 4^+ level at 2329.0 keV and a 2^+ level at 2365.4 keV. Four new levels were discovered at 2507.6, 2698.0, 2825.2, and 2859.8 keV respectively. Eighteen angular distributions of γ rays from the ^{94}Zr levels through 2887.7 keV were measured at 3.10-MeV neutron energy, and γ-ray branching ratios were determined. As in the measurements for ^{92}Zr, the WHF calculations were in excellent agreement with measured angular distributions for decays from 6 low-lying excited levels of known spin and parity. For higher levels, the analysis of these angular distributions resulted in the unique or limiting spin and parity assignments given in Table VI and Fig. 2. Based on our own results, we have made unique assignments to the following three levels in ^{94}Zr (E_x in keV, J^π): 2365.4, 2^+; 2507.6, $3^{(+)}$; 2603.7, (5). Combining our information with results from other laboratories gives the following assignments or limitations: 2329.0, 4^+; 2365.4, 2^+; 2507.6, $3^{(+)}$; 2603.7, 5^-; 2698.0, 0^+, 1–3; 2825.2, 2, 3; 2846.0, 1, 2; 2859.8, $4^{(-)}$, 5; 2887.7, 0^+, 1–3; and 3155.5, 4^+. The γ-ray multipole mixing ra-

tios were obtained from our analysis for the acceptable spin possibilities. (Preferred assignments are underlined above.)

With the discovery of the probable 4^- level at 2859.8 keV in ^{94}Zr, and the confirmation of 5^- and 4^- assignments to the 2485.1- and 2742.6-keV levels in ^{92}Zr, one can see the 5^-, 4^- proton excited doublet in the three Zr isotopes with $A = 90$, 92, and 94. The centroid energy of the doublet changes very little with A, increasing only 200 keV from ^{90}Zr to ^{94}Zr. This remarkable stability reflects the fact that the $g_{9/2}$ shell, the valence proton shell, is full for neutrons. Since valence neutron shells are all even parity up to quite large excitation energies, odd-parity neutron configurations are not available. However, there is an evolution in the decay behavior of the 4^- levels with increasing N. In ^{90}Zr the 4^- appears to decay only with a fast $M1$ to the 5^- level.[30] However, in ^{92}Zr an $E1$ decay to the first 4^+ level competes favorably with the $M1$, and in ^{94}Zr the only mode of decay is apparently by an $E1$ transition.

Other than the stability of the excitation energies of the proton-excited doublets, there is another indication of the constancy of the proton configurations in these Zr isotopes. Measurements of the $E2/M1$ mixing ratios for the $2_2^+ \rightarrow 2_1^+$ transition in both of them yield very similar values, $\delta = +0.13 \pm 0.05$ for ^{92}Zr and $+0.22 \pm 0.1$ for ^{94}Zr. Krane has shown[61] that these ratios can be treated as the result of the proton contributions to the low-lying levels, and has successfully calculated δ for ^{92}Zr on that basis. The similar δ's found here for the two isotopes are consistent with essentially the same proton configuration for both.

The neutron inelastic scattering cross sections inferred from the results of the 3.20-MeV ^{92}Zr $(n,n'\gamma)$ angular distribution study have been used with the ^{92}Zr$(n,n'\gamma)$ excitation functions to obtain inferred neutron inelastic scattering cross sections at several neutron energies. The inferred inelastic cross sections agree with those measured directly[28,31,60] in (n,n') experiments to within the combined uncertainties for both types of measurements. The consistency supports the confidence with which these uncertainties are quoted.

APPENDIX A

It has been pointed out by Smith *et al.*,[62] by Beghian and Kegel,[63] and others that fluctuations in the excitation function for neutron scattering to the 847-keV first excited level of ^{56}Fe tend to make use of that reaction for cross section normalization subject to large uncertainties. In this experiment these fluctuation effects are minimized by the following:

(1) Our use of ^{56}Fe$(n,n'\gamma)$ ^{56}Fe measurements[44,45] averaged over an incident energy spread of 60 keV, the spread used in the present experiment. This averaging interval is large compared to the energy width of fluctuations observed in high resolution ^{56}Fe$(n,n'\gamma)$ experiments.[64]

(2) Fluctuations in the cascade contributions to the 847-keV transition from higher levels are incoherent for the various cascade chains. These contributions dominate the 847-keV production cross section above 2.5-MeV incident energy, so the structure in the ^{56}Fe$(n,n'\gamma)$ cross section is much less than that in the ^{56}Fe(n,n') cross section.

APPENDIX B

Beer[52] has made a compilation of all γ-ray transitions which are known to have an $M2$-$E1$ mixture in order to investigate possible systematics in the mixing. There are 116 transitions in the compilation and of these, only 7 transitions have a mixing ratio $\delta > 0.50$ and 4 transitions have a mixing ratio $\delta \geq 1.00$. There are no transitions with $\delta \geq 0.3$ for decaying nuclei in the mass region $60 \leq A \leq 125$. Based in part on these results, we have adopted the criterion for ^{92,94}Zr that for a mixed $L = 1$, 2 transition, the mixture must be $M1$-$E2$ if $\delta \geq 1.00$. For transitions where the final state parity is known, this criterion fixes the parity of the decaying state.

---

*Work supported in part by the National Science Foundation.

†Now at Mallinckrodt Institute of Radiology, Washington University, St. Louis, Missouri.

‡Now at Dept. of Physics, North Texas State University, Denton, Texas.

§On leave at Los Alamos Scientific Laboratory, Los Alamos, New Mexico.

[1]F. D. McDaniel, G. P. Glasgow, J. D. Brandenberger, J. L. Weil, and M. T. McEllistrem, Bull. Am. Phys. Soc. 18, 722 (1973); G. P. Glasgow, F. D. McDaniel, J. D. Brandenberger, J. L. Weil, and M. T. McEllistrem, *ibid.* 18, 1416 (1973); *Proceedings of the International Conference on Nuclear Structure and Spectroscopy*, edited by H. P. Blok and A. E. L. Dieperink (Scholar's Press, Amsterdam, 1974), p. 91.

[2]D. C. Kocher and D. J. Horen, Nucl. Data Sheets B7, 299 (1972).

[3]J. G. Beery, Los Alamos Scientific Laboratory Report No. LA-3958, 1968 (unpublished); E. R. Flynn, J. G. Beery, and A. G. Blair, Nucl. Phys. A218, 285 (1974).

[4]J. B. Ball, R. L. Auble, and P. G. Roos, Phys. Rev. C 4, 196 (1971).

[5]C. R. Bingham and M. L. Halbert, Phys. Rev. C 2, 2297 (1970).

[6]B. L. Berman and R. J. Baglan, J. Inorg. Nucl. Chem.

31, 9 (1969); W. L. Talbert, Jr., F. K. Wohn, H. H. Hsu and S. T. Hsue, Nucl. Phys. A146, 149 (1970).
[7]E. R. Flynn, D. D. Armstrong, and J. G. Beery, Phys. Rev. C 1, 703 (1970).
[8]M. M. Stautberg, and J. J. Kraushaar, Phys. Rev. 151, 969 (1966); K. Matsuda, H. Nakamura, I. Nonaka, H. Taketani, T. Wada, Y. Awaya, and M. Koike, J. Phys. Soc. Japan 22, 1311 (1967).
[9]J. K. Dickens, E. Eichler, and G. R. Satchler, Phys. Rev. 168, 1355 (1968).
[10]R. K. Jolly, E. K. Lin, and B. L. Cohen, Phys. Rev. 128, 2292 (1962).
[11]U. Fanger, D. Heck, R. Pepelnik, H. Schmidt, and J. Wood, *International Conference on Nuclear Structure Study With Neutrons*, (Karlsruhe, Germany, 1972), pp. 72 and 73.
[12]J. L. Wood, Center for Nuclear Research, Karlsruhe, Germany, External Report No. 1/72-1, 1972 (unpublished), pp. 32 and 33.
[13]D. C. Kocher, Nucl. Data Sheets 10, 241 (1973).
[14]G. Tessler, S. S. Glickstein, and E. E. Carroll, Jr., Phys. Rev. C 2, 2930 (1970).
[15]G. Tessler and S. Glickstein, Phys. Rev. C 6, 1430 (1972).
[16]R. B. Day, in Neutron Cross Sections, compiled by M. D. Goldberg, S. F. Mughabghab, B. A. Magurno, and V. M. May, Brookhaven National Laboratory Report No. BNL-325, 2nd ed., Supp. No. 2, Vol. IIA (unpublished); R. B. Day and D. A. Lind, unpublished data partially reported by R. B. Day, in *Progress in Fast Neutron Physics*, edited by G. C. Phillips, J. B. Marion, and J. R. Risser (The University of Chicago Press, Chicago, 1963).
[17]P. Cavallini, S. André, E. Monnand, and F. Schussler Nucl. Phys. A175, 370 (1971).
[18]S. Hontzeas and D. A. Marsden, Nucl. Phys. A179, 198 (1972).
[19]B. Singh, H. W. Taylor, and P. J. Tivin, J. Phys. G2, 397 (1976).
[20]K. C. Chung, A. Mittler, J. D. Brandenberger, and M. T. McEllistrem, Phys. Rev. C 2, 139 (1970).
[21]S. Cohen, R. D. Lawson, M. H. MacFarlane, and M. Soga, Phys. Lett. 10, 195 (1964): J. Vervier, Nucl. Phys. 75, 17 (1966).
[22]D. H. Gloeckner and F. J. D. Serduke, Nucl. Phys. A220, 477 (1974).
[23]J. B. Ball, J. B. McGrory, and J. S. Larson, Phys. Lett. 41B, 581 (1972).
[24]J. S. Larsen, J. B. Ball, and C. B. Fulmer, Phys. Rev. C 7, 751 (1973).
[25]D. H. Gloeckner, Nucl. Phys. A253, 301 (1975).
[26]M. T. McEllistrem, J. D. Brandenberger, K. Sinram, G. P. Glasgow, and K. C. Chung, Phys. Rev. C 9, 670 (1974).
[27]F. D. McDaniel, J. D. Brandenberger, G. P. Glasgow, and H. G. Leighton, Phys. Rev. C 10, 1087 (1974).
[28]F. D. McDaniel, J. D. Brandenberger, M. T. McEllistrem, K. Sinram, and G. P. Glasgow, Bull. Am. Phys. Soc. 18, 1402 (1973).
[29]K. Sinram, K. C. Chung, J. D. Brandenberger, and M. T. McEllistrem, Bull. Am. Phys. Soc. 15, 1692 (1970); J. D. Brandenberger, K. C. Chung, K. Sinram, G. P. Glasgow, C. E. Robertson, and M. T. McEllistrem, *ibid.* 16, 1181 (1971); K. Sinram, J. D. Brandenberger, and M. T. McEllistrem, *ibid.* 17, 901 (1972)
[30]S. S. Glickstein, G. Tessler, and M. Goldsmith, Phys. Rev. C 4, 1818 (1971). S. S. Glickstein and G. Tessler, *Proceedings of the Third Conference on Neutron Cross Sections and Technology*, edited by R. L. Macklin (USAEC-DTIE, Oak Ridge, Tenn. 1971), Vol. 1, p. 241; G. Tessler and S. Glickstein, *Proceedings of Nuclear Cross Sections and Technology*, NBS Spec. Pub. No. 425, edited by R. A. Schrack and C. D. Bowman (U. S. Government Printing Office, Washington, D. C., 1975), Vol. II, p. 934.
[31]P. Guenther, A. Smith, and J. Whalen, Phys. Rev. C 12, 1797 (1975).
[32]G. P. Glasgow, K. Sinram, J. D. Brandenberger, and M. T. McEllistrem, Bull. Am. Phys. Soc. 17, 901 (1972).
[33]J. D. Brandenberger, Nucl. Instrum. Methods 69, 271 (1969).
[34]S. Gorni, G. Hochner, E. Nadav, and H. Zmora, Nucl. Instrum. Methods 53, 349 (1967); J. P. Fouan and J. P. Passerieux, *ibid.* 62, 327 (1968).
[35]J. T. Routi and S. G. Prussin, Nucl. Instrum. Methods 72, 125 (1969).
[36]J. T. Routi, University of California Lawrence Radiation Laboratory Report No. UCRL-19542, 1969 (unpublished).
[37]G. Aubin, J. Barrette, M. Barrette, and S. Monaro, Nucl. Instrum. Methods 76, 93 (1969); L. J. Jardine, *ibid.* 96, 259 (1971); J. B. Marion, Nucl. Data A4, 312 (1968).
[38]C. A. Engelbrecht, Nucl. Instrum. Methods 80, 187 (1970); C. A. Engelbrecht, *ibid.* 93, 105 (1971).
[39]J. W. Boring, Ph.D. dissertation, University of Kentucky, 1960 (unpublished).
[40]E. Storm and H. I. Israel, Nucl. Data A7, 565 (1970); W. H. McMaster, N. K. Del Grande, J. H. Mallett, and J. H. Hubbell, University of California Lawrence Radiation Laboratory Report No. UCRL-50174 (Sec. 2) (Rev. 1), 1969 (unpublished), p. 161.
[41]D. Broerman and C. J. Paperiello, University of Notre Dame Nuclear Spectroscopy Group Internal Report, 1968 (unpublished).
[42]J. F. Emery and M. A. Lepri, Oak Ridge National Laboratory Report No. ORNL-4343, 1968 (unpublished), p. 73; J. B. Marion, Nucl. Data A4, 301 (1968).
[43]H. Seyrarth, Nucl. Instrum. Methods 105, 378 (1972).
[44]T. Looney and M. T. McEllistrem, (unpublished). Also see Ref. 60.
[45]M. T. McEllistrem, in *Nuclear Research with Low Energy Accelerators*, edited by J. B. Marion and D. M. Van Patter (Academic, New York, 1967), pp. 167 and 168.
[46]L. Wolfenstein, Phys. Rev. 82, 690 (1951); W. Hauser and H. Feshbach, *ibid.* 87, 366 (1952).
[47]E. Sheldon and D. M. Van Patter, Rev. Mod. Phys. 38, 143 (1966)); E. K. Warburton, J. W. Olness, and A. R. Poletti, Phys. Rev. 160, 938 (1967).
[48]P. R. Bevington, *Data Reduction and Error Analysis for the Physical Sciences* (McGraw-Hill, New York, 1969).
[49]N. C. Francis, Knolls Atomic Power Laboratory, private communication.
[50]E. H. Auerbach, N. C. Francis, D. T. Goldman, and C. R. Lubitz, Knolls Atomic Power Laboratory Report No. KAPL-3020, 1964 (unpublished).
[51]H. J. Rose and D. M. Brink, Rev. Mod. Phys. 39, 306

(1967).
[52]S. K. Beer and A. P. Arya, Bull. Am. Phys. Soc. 21, 640 (1976); S. K. Beer, M. S. thesis, West Virginia University, 1976 (unpublished).
[53]L. Dresner, *Proceedings of International Conference on the Neutron Interaction with the Nucleus* TIO-7547, edited by W. W. Havens (USAEC-DTIE, Oak Ridge, Tenn., 1957), p. 71 and A. M. Lane and J. B. Lynn, Proc. Phys. Soc. London 70, 557 (1957).
[54]P. A. Moldauer, Phys. Rev. 123, 968 (1961); 129, *ibid.* 754 (1963); *ibid.* 135, B642 (1964); Rev. Mod. Phys. 36, 1064 (1964).
[55]M. E. Bunker, B. J. Dropesky, J. D. Knight, and J. W. Starner, Phys. Rev. 127, 844 (1962).
[56]R. P. Chestnut, F. E. Cecil, and R. L. McGrath, Phys. Rev. C 10, 2434 (1974).
[57]G. P. Glasgow, Ph.D. dissertation, University of Kentucky, 1973 (unpublished).
[58]H. Singh, V. K. Tikku, B. Sethi, and S. K. Mukherjee, Radio-chem. and Radioanal. Lett. 15, 201 (1973).
[59]S. Raman and N. B. Gove, Phys. Rev. C 7, 1995 (1973).
[60]F. D. McDaniel, (unpublished).
[61]K. S. Krane, Phys. Rev. C 10, 1197 (1974).
[62]A. B. Smith, J. F. Whalen, and K. Takeuchi, Phys. Rev. C 1, 581 (1970).
[63]Leon E. Beghian and G. H. R. Kegel, progress report, Lowell Technological Institute, Lowell, Mass., 1972 (unpublished).
[64]G. T. Chapman, J. K. Dickens, T. A. Love, G. L. Morgan, and E. Newman, Bull. Am. Phys. Soc. 20, 166 (1975); V. C. Rogers, V. J. Orphan, C. G. Hoot, V. V. Verbinski, D. G. Costello, and S. J. Friesenhahn, *ibid.* 20, 166 (1975).